

Spectrally Resolved Dynamics of Energy Transfer in Quantum-Dot Bilayers **IHRP**

Achermann, M., LANL
Hollingsworth, J.A., LANL
Petruska, M.A., LANL
Klimov, V.I., LANL
Crooker, S.A., NHMFL/LANL
Tretiak, S., LANL

Communication and coupling between quantum dots (QDs) are central themes in numerous scientific efforts of present physical and technological interest. A promising approach exploits the readily achievable coupling via incoherent long-range dipolar interactions, which allow interdot communication via Förster energy transfer (ET). The ET rate $\Gamma_{ET} \propto \Theta R_{DA}^{-6}$ depends on the spectral overlap Θ between donor emission and acceptor absorption line shapes and is very sensitive to the donor-acceptor distance R_{DA} . Good spectral overlap between semiconductor nanocrystal QDs is obtained between dots of different sizes as a result of the global Stokes shift between QD absorption and emission (Figure 1(a)).

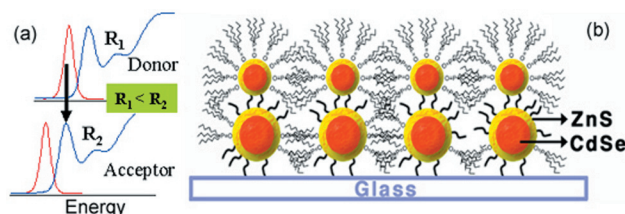


Figure 1. (a) Schematic of non-radiative Förster energy transfer between nanocrystal QDs. Due to the energy shift of emission and absorption, efficient ET occurs only from small to large QDs. (b) Design of the bilayer structure, which consists of a large and a small monolayer of ZnS capped CdSe QDs.

We designed a prototype bilayer light harvesting structure out of CdSe nanocrystal QDs. Assembling a monolayer of small dots on top of a monolayer of large dots, we expect efficient vertical energy transfer from small to large dots due to efficient coupling of the small dot emission to the high energy absorption of the large dots (Figure 1(b)). After exciting the QD bilayer sample with a short laser pulse, time-resolved photoluminescence (PL) measurements allow us to follow the excitation energy in time.¹ Figure 2(a) shows the PL spectra at different time delays Δt after excitation. The spectra are normalized to equal spectral areas to compensate for radiative and non-radiative losses and therefore to reveal directly energy

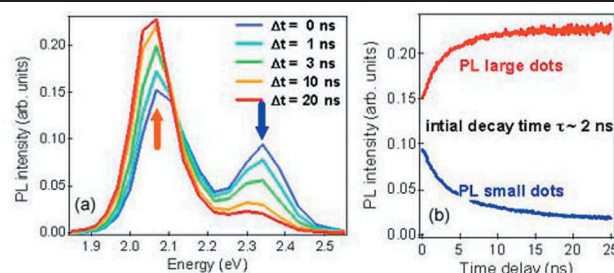


Figure 2. (a) PL spectra taken from the bilayer structure at different time delays after laser excitation. The decrease of the high energy peak (small QDs) and the increase of the low energy peak (large QDs) are associated with energy transfer from small to large QDs. (b) Time traces of the PL signal taken at the energies indicated in (a). The measured dynamics reveal an energy transfer time of 2 ns.

transfer processes. The spectra show two peaks accounting for the emission of the two monolayers with different size QDs. We find that the high energy peak (small QDs) decays rapidly, whereas the low energy peak (large QDs) increases with time. This is a direct evidence for energy transfer from small to large QDs. From time traces taken at the maxima of the two peaks (Figure 2(b)) we determine an ET time of as short as 2 ns. The energy transfer in this bilayer structure is not only fast but also efficient. We calculate that 50% of the excitation moves from the small to the large dots within the lifetime of the excitation (limited by the radiative recombination of 20 ns).

¹ Crooker, S.A., *et al.*, *Phys. Rev. Lett.*, **89**, 186802 (2002).

Magnetotransport in Ferromagnetic CaB_6

Aronson, M., Univ. of Michigan, Physics
Bennett, M., Univ. of Michigan, Physics
Berkeley, E., Univ. of Michigan, Physics
Balakirev, F., NHMFL/LANL
Fisk, Z., NHMFL

The discovery of weak ferromagnetism with very high Curie temperatures in the doped alkali earth hexaborides was remarkable. While there is little debate that stoichiometric CaB_6 is a nonmagnetic semiconductor, much less is known about how the magnetic and electronic properties develop as a function of electron or hole concentration. It is the aim of our work to provide this information, particularly in samples with much lower carrier concentrations than have previously been studied.

We have studied 16 different samples of CaB_6 , using Hall effect, electrical resistivity, and magnetization

SEMICONDUCTORS

measurements. The Hall voltage is linear in fields as large as 60 T, revealing that electron doping is dominant in our samples, at concentrations which range from 9×10^{17} to $7 \times 10^{19} \text{ cm}^{-3}$. Weak magnetic freezeout, at the level of 10%, is observed in the most lightly doped samples at the lowest temperatures, and above ~ 20 T. We find that the samples transform from metallic to insulating when the electron concentration drops below $\sim 8 \times 10^{18} \text{ cm}^{-3}$, accompanied by a dramatic increase in the spontaneous magnetization. In this insulating and magnetic phase, it is possible to approach the quantum limit, $\omega_c \tau = 1$, in the fields available at the NHMFL-LANL, and this was the motivation for the experiments that we carried out in the summer of 2002.

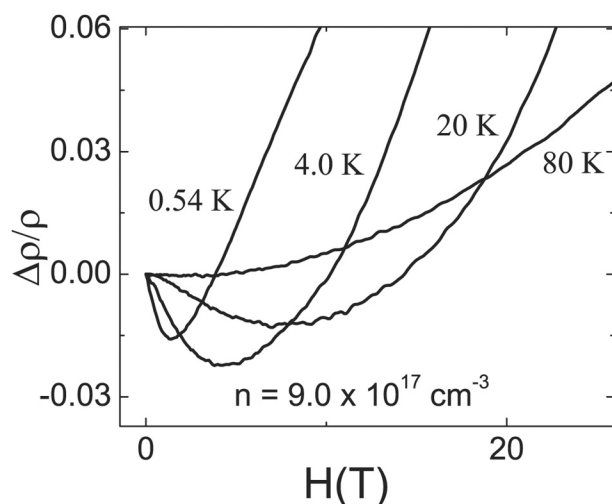


Figure 1. The longitudinal magnetoresistance of a CaB_6 sample doped to lie near the insulator-metal transition. These data were obtained in the 50 T medium pulse magnet, using the dual direct digital synthesizer.

We carried out measurements of the longitudinal resistivity on CaB_6 samples with carrier concentrations that spanned the magnetic phase diagram, i.e. both metallic and insulating. At every concentration, we found that the magnetoresistance was initially negative in low fields, attaining a minimum value at a field that depends on the sample magnetization, before becoming positive in high fields. An example of our results is shown in Figure 1, which further demonstrates the rapid increase in both the positive and negative components of the magnetoresistance with reduced temperature. As indicated in Figure 2, the high field magnetoresistance displays the same asymptotic field dependence in every sample, proportional to H^3 . We propose that this is the orbital magnetoresistance, and that it reveals an underlying electronic structure that is common to each electron concentration. The origin of the negative magnetoresistance is more controversial. We find that the negative magnetoresistance is largest in the samples with the largest moments, suggesting that it

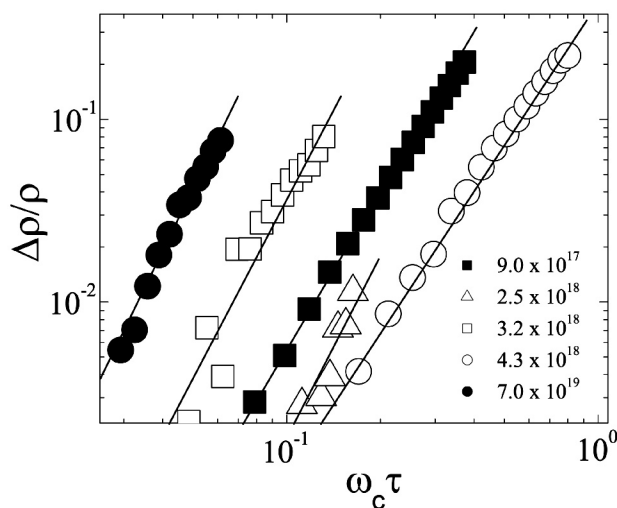


Figure 2. The positive longitudinal magnetoresistance at high field is shown for samples with different electron concentrations at 0.5 K. The solid lines are power law fits to the data, and have slopes of approximately 3 in each case.

originates from spin disorder scattering. These field and temperature dependences are quite unexpected, however, given the anticipated magnitude of the Curie temperatures and the observed saturation of the low field magnetization.

Singlet and Triplet States of Charged Excitons in High Magnetic Fields

Astakhov, G.V., Physikalisches Institut der Universität Würzburg, Germany

Yakovlev, D.R., Experimentelle Physik 2, Universität Dortmund, Germany

Crooker, S.A., NHMFL/LANL

Ossau, W., Physikalisches Institut der Universität Würzburg, Germany

Low-temperature optical (reflectivity and photoluminescence) studies of negatively (X^-) and positively (X^+) charged excitons (trions) have been carried out in collaboration with University of Würzburg (Germany). Detailed overview of the trion appearance in optical spectra of ZnSe-based QWs can be found in Reference 1. The studied structures are ZnSe/(Zn,Be,Mg)Se or ZnSe/(Zn,Mg)(S,Se) single quantum wells (SQW) of 67 Å or 105 Å width. They are lightly doped to produce very dilute 2D electron or hole gases (2DEG or 2DHG) with density below 10^{10} cm^{-2} , which allows us to study the properties of “isolated” trions. The aim of these studies was to perform a detailed analysis of the fine structure of trions. In weak magnetic fields only a *singlet state* of the charged exciton with an antiparallel orientation of electron (or hole) spins is observed. High

magnetic fields above 15 T are required to stabilize a *triplet state* with electron (hole) spins being oriented in a same direction.

During this study it was found that the binding energy of the singlet state of negatively (X^-) and positively (X^+) charged excitons reveals qualitatively different behavior. The former slightly decreases, while the later significantly increases with growing magnetic fields. Such different behavior arises from the different wave functions of negatively and positively charged excitons. Whereas the X^- consists of two light particles (electrons) bound to one heavy particle (hole), the X^+ is constructed of two heavy particles and one light particle moving between these two centers. In the first case, magnetic fields push the electron wave functions closer to the hole, inducing an increase of X^- binding energy. In the second case, applied magnetic fields obstruct the optimal movement of the electron around the two holes, resulting in a decrease of the X^+ binding energy.

The triplet state of the charged exciton appears in magnetic fields above 15 T as a low-energy shoulder of a neutral exciton, as was predicted by a theory. In fields higher then 30 T the binding energy of triplet state may exceed that of the singlet states (see Figure 1). Careful analysis of optical spectra in this range of magnetic field shows that an anticrossing of singlet and triplet states occurs (as shown in the figure). This result is rather unexpected because the wave functions of singlet and triplet states are constructed to be orthogonal. The observation of anticrossing means that a spin-dependent interaction should be taken into account in order to mix these states.

In order to examine singlet-triplet interaction inside of charged exciton in different systems, CdTe/(Cd,Mg)Te SQWs containing dilute 2DEG were used for similar

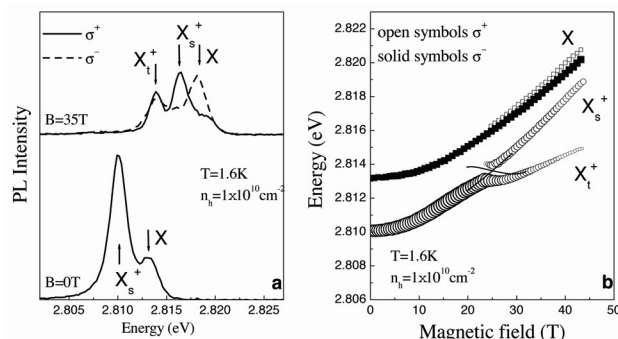


Figure 1. (a) PL spectra of 105 Å thick ZnSe/(Zn,Mg)(S,Se) containing 2DHG of low density measured in zero magnetic field and in magnetic field of 35 T. (b) The energy of neutral exciton X (shown both σ^+ and σ^- circular components), and energy of singlet and triplet states of positively charged exciton (shown only σ^+ circular polarization) as function of magnetic field.

studies. In contrast to the case of ZnSe-based QWs, both “dark” and “bright” configurations (arising from total-angular-momentum selection rule) of triplet states are available to detected separately in photoluminescence spectra of CdTe-based QWs. Careful analysis of experimental data as well as theoretical consideration are required to clarify the problem of singlet-triplet anticrossing. While the former is going on intensively now, the later is in plans.

Results of this project have been presented in three invited talks by W. Ossau at NATO Workshop on “Optical properties of 2D systems with interacting electrons,” June 2002, St. Petersburg, Russia; by D.R. Yakovlev at 15th International Conference on High Magnetic Fields in Semiconductor Physics, August 2002, Oxford, UK; and by G.V. Astakhov at the International Seminar in Würzburg on 3rd International Workshop on II-VI Heterostructures, October 2002, Wuerzburg, Germany. Some of the results are included in the referenced publications.^{1,2,3}

- ¹ Astakhov, G.V., *et al.*, *Phys. Rev. B*, **65**, 165335-17 (2002).
- ² Astakhov, G.V., *et al.*, Proc. of the 26th International Conference on the Physics of Semiconductors, Edinburgh, UK, 29 July - 2 August, 2002, Published by IoP, in press.
- ³ Ossau, W., *et al.*, Proc. of NATO Advanced Research Workshop “Optical Properties of 2D Systems with Interacting Electrons,” St. Petersburg, Russia, 13-16 June, 2002, in press.

Decrease of Oscillator Strength in High Magnetic Field for Pinning Mode Resonance of 2D Electron System **IHRP**

Chen, Y., NHMFL/Princeton Univ., Electrical Engineering
Lewis, R.M., NHMFL/Princeton Univ., Electrical Engineering

Engel, L.W., NHMFL

Tsui, D.C., Princeton Univ., Electrical Engineering
Pfeiffer, L.N., Bell Laboratories, Lucent Technologies
West, K.W., Bell Laboratories, Lucent Technologies

Two-dimensional electron systems (2DES) of sufficient quality exhibit a microwave resonance in the insulating phase that terminates the series of fractional quantum Hall states at the high magnetic field (B). This insulator is thought to be a form of pinned Wigner crystal (WC), and the resonance is interpreted as a pinning mode, in which WC domains oscillate in the pinning potential.

We studied a sample with carrier density (n) tunable over a wide range (7.7 to $1.3 \times 10^{10} \text{ cm}^{-2}$) *in situ* by application of backgate voltage, in B up to 33 T. Figure 1 shows peak frequency, f_{pk} , and integrated intensity (oscillator

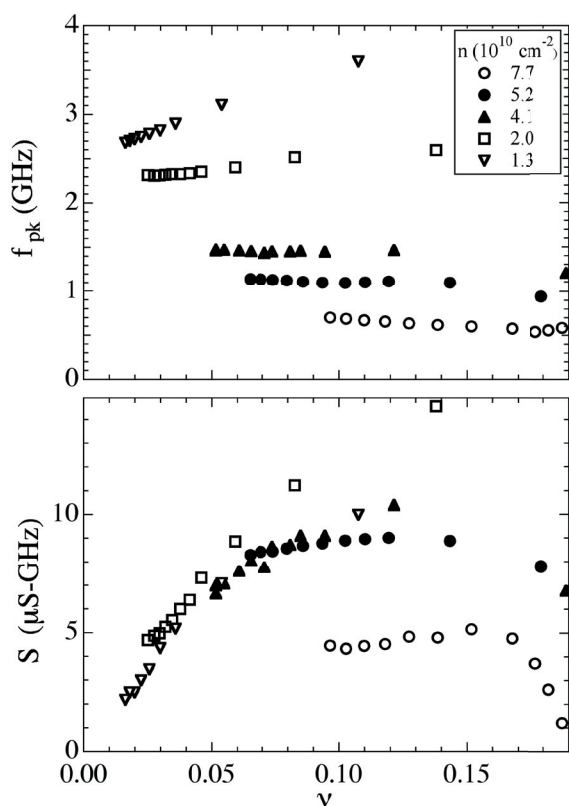


Figure 1. (a) Resonance peak frequency, f_{pk} , vs. Landau filling ν , for various carrier densities, n . (b) resonance oscillator strength, S , vs. ν . Densities and their symbols as in (a).

strength, S) vs. Landau filling ν , for several different n 's. Particularly for the lowest n 's, but in general for $\nu < 0.13$, S decreases with decreasing ν , a behavior not seen previously. As ν decreases, f_{pk} decreases for smaller n , but increases slightly for larger n . f_{pk} and S vs. ν (for fixed n), were predicted long ago¹ to go as ν and ν^2 respectively. The present data indicate the situation is more complicated, and even when f_{pk} and S both decrease with decreasing ν , they do not change as rapidly as was predicted. f_{pk} can be converted² to a correlation length of WC order, or domain size (L). For low n 's L vs. ν fits $L = L_0 + \beta\nu$ over considerable ranges of ν , up to a factor of five, as described in detail in Reference 2.

¹ Fukuyama, H., *et al.*, *Phys. Rev. B*, **17**, 535 (1978).

² Ye, P.D., *et al.*, *Phys. Rev. Lett.*, **89**, 176802 (2002).

Intrinsic Limits to the Dark Exciton Lifetime in CdSe Nanocrystal Quantum Dots **IHRP**

Crooker, S.A., NHMFL/LANL

Barrick, T., NHMFL/LANL

Hollingsworth, J., LANL

Klimov, V.I., LANL

The intense interest in colloidal semiconductor nanocrystal quantum dots (NQDs) derives in part from their size-tunable optical properties and the ease of chemical manipulation into structures of varied complexity for a "bottom-up" approach to both small- and large-scale nano-assemblies.

Particularly noteworthy for device applications are the very large photoluminescence (PL) quantum yields of high quality NQDs—values of 20 to 50% are routine, and recent reports of 85% quantum yield at 300 K indicate the nearly complete absence of nonradiative decay mechanisms. As such, measurements of PL decay directly yield the intrinsic *radiative* lifetime of charge (electron-hole) excitations, a fundamental property of any nanometer-scale semiconductor system. In NQDs it is known, particularly in well-studied wurtzite CdSe dots, that the low-temperature radiative lifetime τ_r far exceeds that of their bulk counterpart ($\tau_r \sim 1 \mu\text{s}$, vs. $\sim 1 \text{ ns}$ in bulk CdSe at 4 K). It is established that these long lifetimes result from the dot's intrinsic crystal/shape anisotropy, and confinement-enhanced electron-hole exchange energy. These effects lift the spin degeneracy of the band-edge exciton such that the ground state is, in fact, the exciton with net spin projection $J=2$ (see inset, Figure 1), which is formally forbidden from radiative recombination (photons having spin 1), and is therefore optically inactive. This "dark" ground state lies well below the nearest optically active "bright" ($J=1$) exciton. The bright-dark energy gap, $\Delta=1\text{--}15 \text{ meV}$, scales inversely with NQD size. Thus, in high-quality NQDs, when the thermal energy $k_B T < \Delta$, excitons are largely frozen in the dark state and no remaining decay channels exist. Within this framework, τ_r should increase exponentially with decreasing temperature, raising the intriguing possibility of long-term "storage" of charge excitations in cold NQDs.¹

Figure 1 shows characteristic PL decay curves at selected temperatures from 1.3 nm radius NQDs on a log scale. At the lowest temperature of 380 mK, τ_r is very long (1.13 μs), and little change is observed up to 2 K. Between 2.5 and 90 K, τ_r drops over an order of magnitude from $\sim 900 \text{ ns}$ to 20 ns, and above 100 K, τ_r remains relatively constant.

Terahertz Absorption Spectroscopy of n-Type InSb Near the Field-Induced Metal-Insulator Transition

IHRP

Crooker, S.A., NHMFL/LANL

Sohn, J.-Y., NHMFL/LANL

Indium antimonide is a narrow-gap semiconductor with a very small electron effective mass ($m^* = 0.014 m_0$), where the high-field limit condition $\hbar\omega_c/4\pi R^* \gg 1$ is easily met in modest magnetic fields ($\hbar\omega_c$ is the cyclotron energy and R^* is the effective Rydberg). If the electrons in a sample exhibit metallic behavior, application of a magnetic field reduces the donor effective Bohr radius and, at a critical field, induces a metal-insulator transition.¹ Using recently-developed fiber-coupled antennas for coherent terahertz spectroscopy in high magnetic fields,² we investigate the terahertz absorption of electron-doped indium antimonide in the vicinity of the magnetic field induced metal-insulator transition. The small energy scales in this problem (plasma frequency ~ 500 GHz, cyclotron energy ~ 2000 GHz/T, and donor binding energy ~ 1.8 meV) are ideally suited for study by broadband terahertz techniques.

Figure 1 shows the absorption of linearly polarized terahertz radiation as a function of magnetic field at 5 K. Dark regions correspond to strong absorption. The sample is a 500 micron thick wafer of Te-doped InSb ($n_e = 2 \times 10^{14} \text{ cm}^{-3}$). At zero field, the plasma edge of the electron gas at ~ 550 GHz is evident by the strong absorption at all lower frequencies. With applied magnetic field, the upper

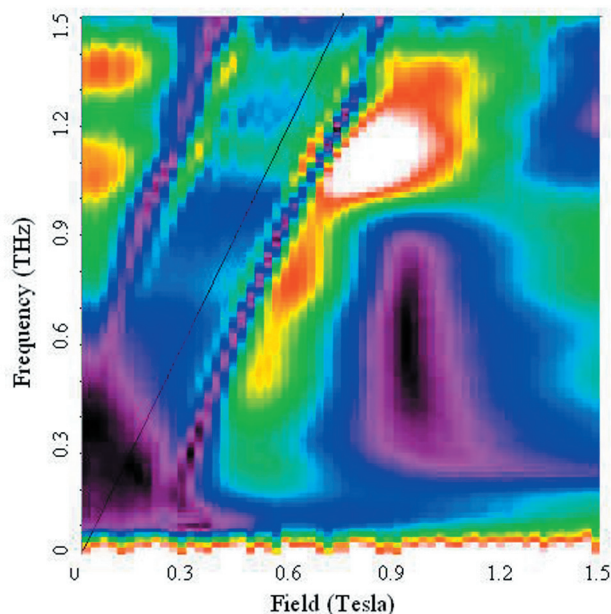


Figure 1. Terahertz absorption of electron-doped InSb at 5 K. Dark regions correspond to strong absorption.

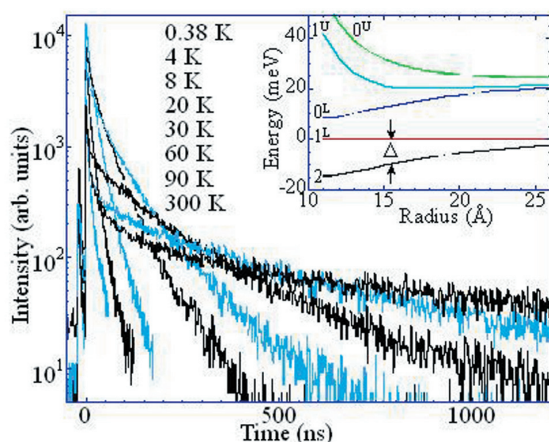


Figure 1. Raw PL decay data (log scale) from 13 nm radius CdSe/ZnS NQDs at the temperatures indicated. Inset: theoretical band-edge exciton spin states vs. NQD size, labeled by the spin projection along the unique crystal axis.

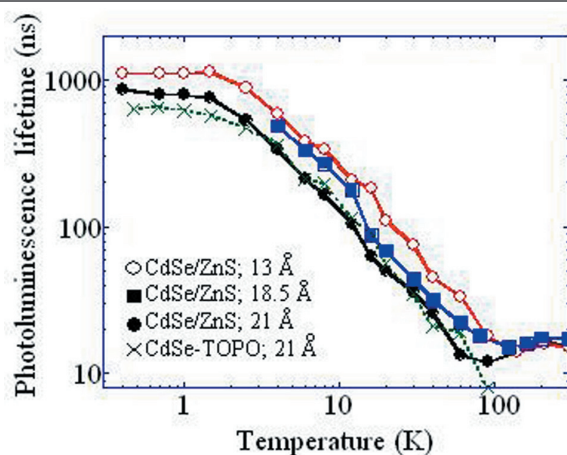


Figure 2. Measured PL lifetimes vs. T (log-log scale) for all NQD samples, showing saturation below 2 K.

Figure 2 shows $\tau_r(T)$ in all the NQD samples, on a log-log scale. Most striking is the low-temperature saturation of τ_r below 2 K, observed in all samples regardless of size or surface passivation. The data do not reflect inadvertent sample heating—a ten-fold increase in laser fluence yielded identical results, and further, 1.5 K data in both liquid ^3He and in superfluid ^4He (where heatsinking is dramatically increased) were the same. The observed lifetime saturation is surprising within the context of a dark-exciton ground state where, as discussed above, τ_r should continue to increase with lower temperatures. Because the overall PL quantum yield does not change appreciably below 20 K (shown below), these data point towards the existence of an intrinsic radiative decay channel which, below 2 K, evidently imposes a fundamental limit of roughly 1 μs on the storage time of electrons and holes in these CdSe NQDs.

¹ Crooker, S.A., *et al.*, *Appl. Phys. Lett.*, **82**, 2793 (2003).

magneto-plasmon absorption moves to higher frequencies, and the collapse of the low frequency absorption is readily seen. The prominent absorption feature that appears to start from zero frequency at finite magnetic field (~ 3000 kG), and moves to higher frequencies with ($\hbar\omega_c \sim 2000$ GHz/T), is not well understood.

Near the critical field at which the metal-insulator transition is expected in this sample ($H_c \sim 9000$ kG), a strong absorption is observed. All frequencies between 250 GHz and 900 GHz are strongly attenuated over a narrow field range about H_c . With increasing field, this region of strong attenuation collapses to a narrow absorption at ~ 300 GHz that persists to 15 T. This region of strong, broadband THz absorption moves to higher magnetic field in samples with increased electron doping, and is significantly less pronounced at elevated temperatures above 10 K. Both of these trends suggest that this feature may be associated with the transition between metallic and insulating behavior. Further studies using crossed THz antennas, to analyze degree of circular polarization, will aid in this ongoing study.

Acknowledgements: This work was supported by the NHMFL In-House Research Program.

¹ Choi, J.B., *et al.*, *Phys. Rev. B*, **43**, 4046 (1991).

² Crooker, S.A., *Rev. Sci. Instr.*, **73**, 3258 (2002).

Theory of the Quantum Hall Nematic

Dorsey, A.T., UF, Physics

Radzihovsky, L., Univ. of Colorado, Physics

Recent measurements of the transport properties of high-mobility two-dimensional electron systems (2DES) have revealed a remarkable phenomenon in the transitional regions between the plateaus of the Hall conductance. In particular, striking anisotropies were observed for higher Landau levels that are close to half-filling. We have developed a theory of this anisotropic phase, which can be thought of as a striped, or “smectic” phase, which is melted due to the proliferation of dislocations; the resulting phase is an anisotropic liquid, or “nematic,” phase of the two-dimensional electrons.

Our model¹ is inspired by the dynamics of the local smectic layers (the so-called chiral edge bosons). From our model we predict a novel collective mode that derives from an oscillation between the orientational degrees of freedom and the electron density. We are able to calculate the tunneling current into this nematic phase and predict a pseudogap in the I-V characteristics. We are currently investigating other experimental ramifications of our model, many of which should be observable at NHMFL

facilities. This work was highlighted in Physical Review Focus: see “Electrons Come to Order,” <http://focus.aps.org/story/v9/st25>.

Acknowledgements: This work was supported in part by NSF Grant No. DMR-9978547.

¹ Radzihovsky, L., *et al.*, *Phys. Rev. Lett.*, **88**, 216802-1-216802-4 (2002).

Searching for Zener Tunneling Effect Between Landau Orbits of Composite Fermions

Du, R.R., Univ. of Utah, Physics

Yang, C.L., Univ. of Utah, Physics

Zudov, M.A., Univ. of Utah, Physics

Pfeiffer, L.N., Bell Laboratories, Lucent Technologies

West, K.W., Bell Laboratories, Lucent Technologies

Zener tunneling between 2D electron Landau orbits is a long sought-after effect in quantum Hall systems. Recently we have discovered a remarkable oscillatory magnetoresistance (R_{xx}) phenomenon in a high-mobility 2D electron gas, observed in a Hall bar sample of GaAs-AlGa_{0.3}As_{0.7} heterostructures or quantum wells. The period of the oscillation (in inverse magnetic field, $1/B$) is proportional to k_F , the electron Fermi wave vector at $B = 0$, and inversely proportional to the current density flowing through the sample. Such effects can be well explained by resonant Zener tunneling between Landau orbits of electrons in a weak B , with a momentum transfer of $2k_F$.

We explored the possible application of such measurements to the composite fermion (CF) regime in a half-filled Landau level² where the Fermi surface effects have been well established but many interesting questions remain open. Because of the selection rules of both momentum and energy, the cyclotron energy (hence, the effective mass) of the CF state could be in principle accessible by this technique. From the Zener tunneling mechanism point of view, since such oscillations require a finite momentum transfer, observation of this effect with CF would allow a look into their short-range interactions.

Preliminary results from a very high-mobility sample are shown in Figure 1. The inset shows sharp oscillations in differential magnetoresistance, r_{xx} , due to Zener tunneling between electronic orbits, in a weak $B < 0.3$ T. The r_{xx} is defined as dR_{xx}/dI at a given bias dc current, I_{dc} . For the same sample, CF orbits are formed around the half-filling ($B \sim 16.8$ T) under an effective magnetic field B_{eff} as labeled by the horizontal axis. With an increasing bias I_{dc} , the r_{xx} around half-filling evolves from sharp high-order

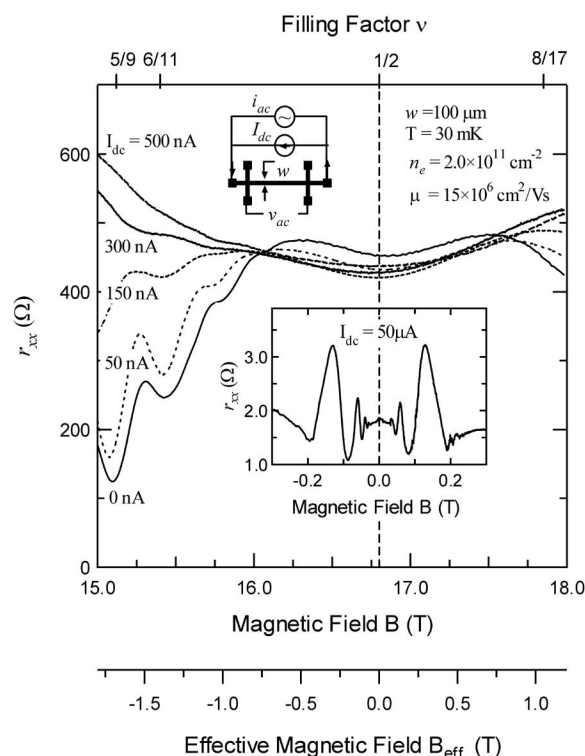


Figure 1. Differential magnetoresistance, r_{xx} , is shown for a high-mobility 2DES around half-filling with increasing bias current, I_{dc} . The inset shows sharp r_{xx} oscillations resulting from Zener resonance of the electron orbits.

fractional quantum Hall states into broad features. With limited data we are unable to characterize such features as resulting from the Zener resonance of CF orbits. We plan to systematically pursue similar experiments at the NHMFL in the future.

¹ Yang, C.L., *et al.*, *Phys. Rev. Lett.*, **89**, 076801 (2002).

² Perspectives in Quantum Hall Effect, edited by S. Das Sarma and A. Pinczuk (Wiley, New York, 1997).

Ferromagnetic Resonance in GaMnAs at Sub-Millimeter Wavelengths

Furdyna, J.K., Univ. of Notre Dame, Physics

Liu, X., Univ. of Notre Dame, Physics

van Tol, J., NHMFL

Brunel, L.-C., NHMFL

GaMnAs has recently been shown to be ferromagnetic semiconductor alloy, with Curie temperatures up to 120 K. This system has recently occupied much of the interest of the scientific community because it holds promise of integration of non-magnetic GaAs-based semiconductor electronics for spintronic applications. The material

is fabricated in thin film form by low-temperature molecular beam epitaxy, with Mn content ranging up to 10 at.%. Since ferromagnetic resonance (FMR) is an extremely powerful tool for investigating the properties of ferromagnetic thin films, we have launched an investigation of this material using this technique.

Multifrequency sub-millimeter FMR capability at NHMFL is particularly attractive for this purpose because it offers the possibility of measuring the effect at several frequencies. This capacity enables the investigator to pin down both the magnetic anisotropy and damping parameters with a minimum of ambiguity. In addition, this approach offers a high degree of resolution of standing spin wave modes in these ferromagnetic thin films. A series of samples with different Mn content were examined at four frequencies as a function of temperature in several field configurations. The resonance data are presently being analyzed.

Photodarkening in Glassy As_2O_3

Hari, P., California State Univ. at Fresno, Physics

Guzel, S., California State Univ. at Fresno, Physics

Taylor, P.C., Univ. of Utah, Physics

Reyes, A.P., NHMFL

Kuhns, P.L., NHMFL

Moulton, W.G., NHMFL

Sullivan, N.S., NHMFL/UF, Physics

Photodarkening, or the shift of the optical absorption edge to smaller energies after excitation with light whose energy is near that of the optical band edge, has been studied in the chalcogenide glasses for many years. We have conducted high field nuclear magnetic resonance (NMR) studies at 17 T and Nuclear Quadrupole Resonance (NQR) studies of ^{75}As in glassy As_2O_3 . We compared the ^{75}As NMR and NQR lineshapes in glassy As_2O_3 before and after irradiation. An increase in the asymmetry parameter would have implied an increase in the departure from cylindrical symmetry in the bonding at the arsenic pyramidal sites. As_2O_3 samples were prepared from arsenolite powder, which was sealed in an evacuated quartz ampoule. The ampoule was heated at 580 C for 6 hours and then quenched in air. Samples were X-irradiated for 15 hours and then placed in shrink-fit tubing and the ends covered with rubber cement. Photodarkening in As_2O_3 was associated with a change in sample color from transparent to orange. High field NMR techniques were performed using the 24.5 T dc magnet at the NHMFL in Tallahassee. Details of the pulsed NMR technique have been published previously^{1,2,3} and will not be repeated here. The important aspect of the present study is that we have used glassy As_2O_3 , which is well known to have a significant shift

in its band edge (of the order of 0.2 eV) upon X-ray irradiation.⁴ The NMR lineshapes of glassy As₂O₃ (Figure 1) indicate that there is no change in the asymmetry of the As sites in the two samples due to photodarkening.

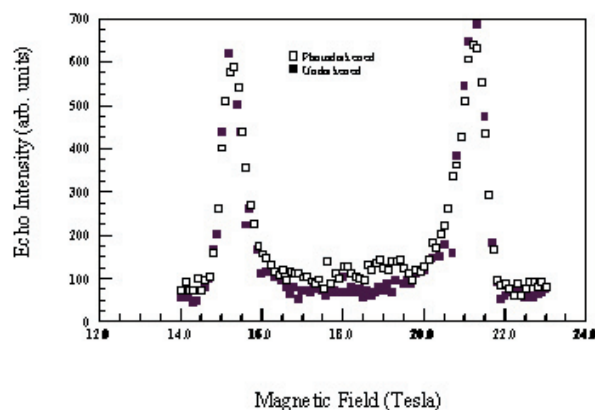


Figure 1. ⁷⁵As NMR lineshape of the central transition in glassy As₂O₃ before (dark squares) and after x-ray irradiation (open squares) is shown. NMR measurements shown here were performed at 131.254 MHz.

A microscopic model^{5,6} of photo structural changes in amorphous selenium has been recently proposed that involves switching of a large number of chalcogen bonds. One of the important questions pertaining to the photodarkening effect in the As-chalcogen could be explained by switching of a large number of As-chalcogen bonds. Switching of large numbers of As-chalcogen bonds in glassy As₂O₃, however, should result in a variation of asymmetry parameter at the As sites, which should result in measurable NMR lineshapes. It is well known⁷ that significant photodarkening extends well into bulk samples at depths up to a mm, albeit at significantly lower levels. Therefore, at least half of the volume should exhibit dramatic effects, especially if there is “bond switching” occurring. From the studies on glassy As₂O₃ we conclude that photodarkening cannot be associated with significant changes in the average symmetry of the As site in these samples. We estimate that changes in the asymmetry parameter of the order of 5% should have resulted in measurable lineshape differences.

¹ Hari, P., et al., *Solid State Commun.*, **104**, 669 (1997).

² Taylor, P.C., et al., *J. Non-Cryst. Solids*, **227**, 770 (1998).

³ Hari, P., et al., *J. Non-Cryst. Solids*, **266**, 929 (2000).

⁴ Tracey, D.J., et al., *Solid State Commun.*, **32**, 423 (1979).

⁵ Kolobov, A.V., et al., *Phys. Rev. Lett.*, **87**, 145502 (2001).

⁶ Kolobov, A.V., et al., *Phys. Rev. B*, **55**, 726 (1997).

⁷ Duschrame, S., et al., *Phys. Rev. B*, **41**, 12250 (1990).

Dynamical Properties of a Luttinger Liquid at the Edge of a Two-Dimensional Electron Gas

Hilke, M., McGill Univ., Physics

Armstrong-Brown, A., McGill Univ., Physics

Engel, L.E., NHMFL

Tsui, D.C., Princeton Univ., Electrical Engineering

West, K.W., Bell Laboratories

Pfeiffer, L.N., Bell Laboratories

A Luttinger liquid arises from the interaction between electrons in one dimension. Because of the reduced dimensionality, interactions are effectively enhanced, which leads to a novel set of properties that only exist in one-dimensional electronic systems.¹ Thanks to a novel fabrication technique, it is possible to realize one-dimensional systems without backscattering.

These systems rely on the peculiar properties of a two-dimensional system at the edge of a sharp boundary under the influence of a large magnetic field. Technically, these structures are obtained by cleaving a GaAs/AlGaAs quantum well along a crystalline axis and by subsequently growing a barrier material in which the height and thickness can be controlled at the atomic level (see illustration in the figure).

When crossing filling factor $\nu=1$ the system shows a Fermi liquid to Luttinger liquid transition and smaller filling factors the Luttinger liquid behavior becomes more and more pronounced, as indicated by the increasingly non-linear tunneling current-voltage characteristic.² In this regime the system can be described by multiple edge modes,¹ where the nature and number of edge modes depends on the filling factor. The idea here is to probe these modes by dynamically exciting them when they are coupled to a high frequency field.

In this work we studied for the first time the tunneling characteristics of the edge of a two-dimensional electron gas and in the presence of very high frequencies and magnetic fields. We fixed our quasi-one-dimensional system onto the microwave strip line, which was placed inside the probe of the dilution refrigerator. In order to maximize the coupling between the Luttinger liquid edge and the microwave signal, we placed the edge along the microstrip of the microwave guide.

In general, we applied a constant DC bias between the two-dimensional electron gas (2DEG) and the edge, which in turns leads to a tunneling current. We measured this tunneling current for various applied microwave fields and magnetic fields. At low microwave powers, i.e., in a regime where we do not induce any heating to our

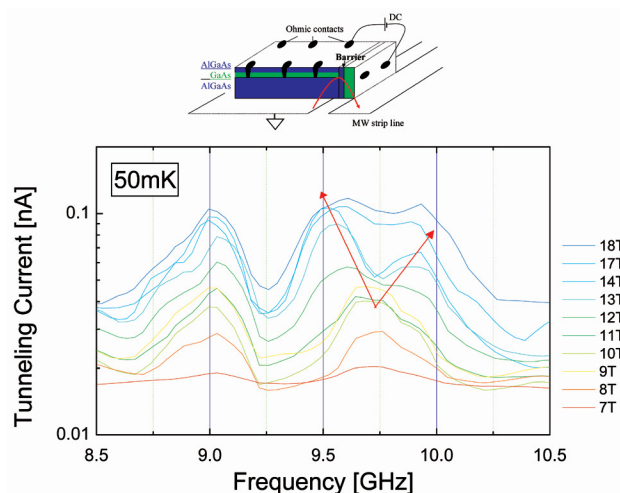


Figure 1. The DC tunneling current between the two dimensional electron gas and the doped edge as a function of applied microwave frequency for different magnetic fields. The curves are obtained by fixing the applied voltage (different for each field) and by measuring the tunneling current.

sample, we observe several tunneling peaks as a function of frequency. Most of the peaks, however, are independent of magnetic field. There is one interesting exception, where we observe the splitting of one tunneling peak at 9.8 GHz at 12 T and all the way up to 18 T as shown in Figure 1. We interpret this splitting as the appearance of an additional mode at the edge of the 2DEG. At 12 T, the filling factor of the 2DEG is $\nu=1/4$, below which this splitting occurs.

Acknowledgements: This work was supported by NSERC, FCAR, NSF, and the NHMFL.

¹ Wen, X.G., *Adv. Phys.*, **44**, 405 (1995).

² Hilke, M., *et al.*, *Phys. Rev. Lett.*, **87** (2001) and references therein.

Metal-Insulator and Glass Transitions in Si MOSFETs in Parallel Magnetic Fields

Jaroszyński, J., NHMFL

Popović, D., NHMFL

Klapwijk, T.M., Delft Univ. of Technology, Applied Physics, The Netherlands

Our previous studies of low-frequency resistance noise have shown that the glassy freezing of a 2D electron system in Si MOSFETs occurs as a precursor to the metal-insulator transition (MIT), i.e. at a density $n_g > n_c$, where n_c is the critical density for the MIT determined from the vanishing of activation energies in the insulating regime.¹ Glass transition is manifested by a sudden and dramatic increase of the noise power S_R , and by a sudden change to the sort of statistics characteristic of complicated multistate systems.^{1,2}

Similar behavior is observed in parallel magnetic fields B of up to 9 T. We find that n_g increases with B , and then saturates for $B \geq 4$ T, analogous to the behavior of $n_c(B)$ (Figure 1). However, the width of the metallic glass phase (MG in Figure 1), $n_c < n_s < n_g$, increases with

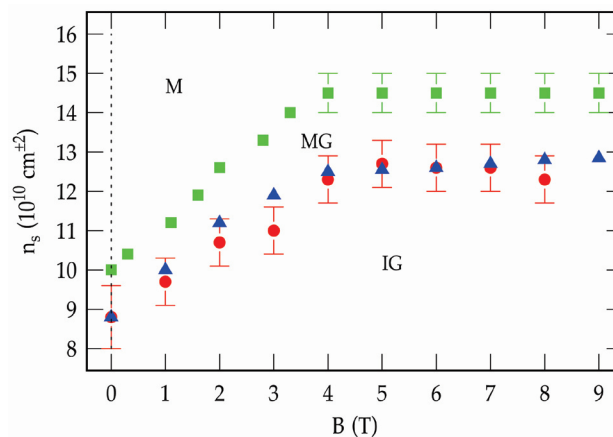


Figure 1. $T = 0$ phase diagram in the (n_s, B) plane. Green squares represent n_g , i.e. densities where the glass transition occurs, and they mark the boundary between metallic (M) and metallic glass (MG) phases. Red dots represent n_c , i.e. critical densities for the metal-insulator transition, and they mark the boundary between metallic glass (MG) and insulating glass (IG) phases. For comparison, blue triangles show the values of n_c (shifted up by 0.8) obtained in Reference 5 on another sample from the same source.

B . This is consistent with theoretical expectations,³ since the effect of B is to suppress the screening and thus increase the effective disorder, which favors glassiness. It is interesting that in the metallic phase, despite positive magnetoresistance, S_R first substantially decreases with B , and then dramatically increases as the system undergoes a B -field driven glass transition at a fixed n_s . For $B > 4$ T,

n_c and n_g no longer depend on B (Figure 1) since the 2D electron system is fully spin polarized at these fields. This indicates that spin degrees of freedom are not responsible for the observed glassy behavior, and that the 2D system freezes into a charge glass, as opposed to a spin glass, in the vicinity of the MIT, in agreement with theory.^{3,4}

Acknowledgements: This work was supported by NSF grant DMR-0071668. We are grateful to V. Dobrosavljević for useful discussions.

- ¹ Bogdanovich, S., *et al.*, *Phys. Rev. Lett.*, **88**, 236401 (2002).
- ² Jaroszyński, J., *et al.*, *Phys. Rev. Lett.*, **89**, 276401 (2002).
- ³ Dobrosavljević, V., *et al.*, *Phys. Rev. Lett.*, **90**, 016402 (2003).
- ⁴ Pastor, A.A., *et al.*, *Phys. Rev. Lett.*, **83**, 4642-4645 (1999).
- ⁵ Shashkin, A.A., *et al.*, *Phys. Rev. Lett.*, **87**, 266402 (2001).

Quantum Hall Ferromagnetism in Diluted Magnetic Semiconductors

Jaroszyński, J., NHMFL

Stringer, E.A., NHMFL and The University of the South, Physics

Popović, D., NHMFL

A giant Zeeman splitting in diluted magnetic semiconductors (DMS) offers a unique opportunity to examine quantum Hall ferromagnetism¹ (QHF) since crossing of Landau levels (LL) can be achieved in moderately strong total magnetic fields ($B \geq 1$ T). This makes it possible to study QHF in a wide range of tilt angles θ . We carried out studies of $\text{Cd}_{1-x}\text{Mn}_x\text{Te}$ quantum wells (QW) with a similar average content of Mn, but with either digital or uniform Mn distribution in the QW. Figure 1 shows that QHF peaks that occur at LL crossings shift toward lower B_{\perp} as θ increases, due to a decrease¹ of the Zeeman gap with increasing B when $B > 1$ T. At the same time, the behavior of the “normal” Shubnikov-de Haas peaks is more complicated, stemming from the redistribution of carriers between overlapping LL and the corresponding shift of

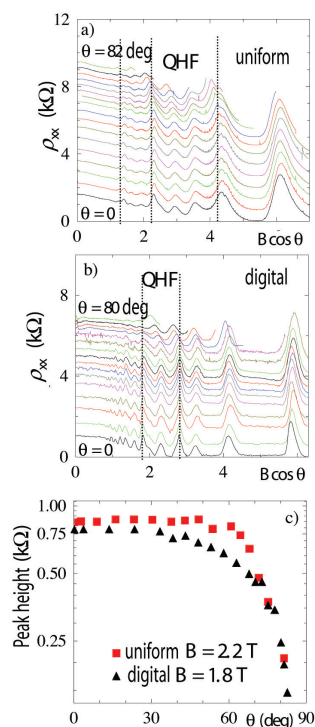


Figure 1. ρ_{xx} resistances at $T=0.330$ K as a function of $B\cos(\theta)$ at different tilt angles θ for a uniform (a) and a digital (b) Mn ion distribution. Vertical dotted lines show positions of the QHF peaks. (c) Amplitudes of the QHF spikes as a function of θ .

the Fermi level. The amplitude of QHF spikes decreases as θ increases, indicating that ferromagnetic domain walls become shorter in a tilted field configuration, with no substantial difference between digitally and evenly doped QW.

The height of the QHF spikes depends dramatically on the history of the sample, shows hysteresis, stretched-exponential time evolution characteristic of glassy systems, and Barkhausen noise reflecting the dynamics of ferromagnetic domains. Our study indicates that these metastabilities stem from the electronic systems itself,² while the changes in the nuclear spin polarization³ play only a minor role. Our results thus corroborate a transition from a stable QHF to a quantum Hall spin glass phase predicted for a sufficiently high disorder.⁴

Acknowledgements: This work was supported by NSF grant DMR-0071668 and the NHMFL. We are grateful to T. Murphy and E. Palm for cryogenic expertise.

- ¹ Jaroszyński, J., *et al.*, *Phys. Rev. Lett.*, **89**, 266802 (2002).
- ² Piazza, V., *et al.*, *Solid State Commun.*, in press (2003).
- ³ Smet, J.H., *et al.*, *Nature*, **415**, 281-286 (2002).
- ⁴ Rapsch, S., *et al.*, *Phys. Rev. Lett.*, **88**, 036801-4 (2002).

Development of an Ultrafast Spectroscopy Facility at the NHMFL for Investigations of Ultrafast Dynamics of Magneto-Excitons

IHRP

Jho, Y.D., UF, Physics

Wei, X., NHMFL

Wang, X., UF, Physics

Kono, J., William Marsh Rice Univ., Electrical and Computer Engineering

Stanton, C.J., UF, Physics

Reitze, D.H., UF, Physics

Excitons in magnetic fields are an ideal system to examine nonlinear and quantum optical phenomena in solid-state systems in a well-controlled manner. The optical field dictates the discrete internal states of excitons, whereas the magnetic field localizes the center-of-mass motion and tunes the internal energy levels. The large spatial extent of excitons results in strong light-matter coupling in the visible and infrared, and dramatic non-perturbative phenomena are expected. The dynamics of excitons in semiconductor quantum structures in the presence of high magnetic fields is a fertile area for exploiting the strong-field analogs of atomic physics in solid-state systems.¹ For example, exploration of the Autler-Townes effect² in quantum-confined systems should answer the fundamental

question as to whether the light excitation in a solid is really quantum, as in quantum optics of atoms. The strong magnetic localization of excitons could lead to the formation of a transient Bose-Einstein condensate at low temperatures that can be probed using ultrafast optical fields.

In order to carry out these investigations, a dedicated facility is required at the NHMFL possessing a broad range of excitation and probe energies. We are developing a time-resolved spectroscopy with 150 fs resolution at fields up to 32 T. Beginning with generation of 775 nm (1.55 eV) laser pulses using a chirped-pulse amplifier followed by optical parametric amplification using optical sum and difference generation, we are able to generate intense 150 fs pulses tunable in the 0.06 to 4.0 eV energy range. Multi-wavelength pump-probe spectroscopy can be accomplished in reflection or transmission in either Faraday or Voigt geometries via specially designed cryostat inserts. In addition, time-resolved photoluminescence can be performed. Figure 1 displays an example of transient absorption spectroscopy under development.

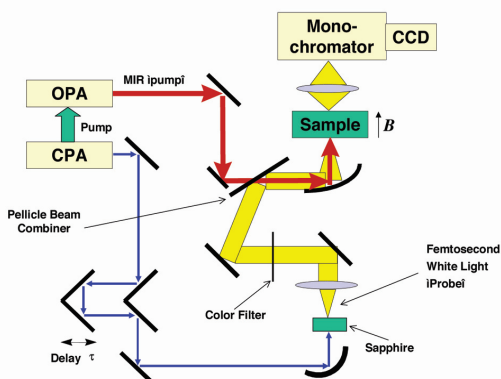


Figure 1. Conceptual schematic of a mid-infrared pump, visible probe transient absorption experiment in the Faraday geometry. A chirped pulse amplifier (CPA) generated 800 nm, 100 fs pulses that pump an optical parametric amplifier (OPA) to generate the mid-IR pump. A visible, time-delayed pulse is created via continuum generation to probe the sample dynamics at a delay time τ after the pump excites the sample.

Time-resolved investigations of magneto-excitons require an understanding of the static magneto-spectroscopy to identify appropriate excitation and probe wavelengths and polarizations. As a prerequisite for our transient spectroscopy experiments, we have studied spin-dependent optical properties of two-dimensional (2D) magneto-excitons in undoped and n-doped $\text{In}_{0.2}\text{Ga}_{0.8}\text{As}$ quantum wells in Faraday and Voigt configurations up to 30 T. In the Faraday configuration using circularly polarized light, we observe strong light-hole - heavy-hole mixing as a function of magnetic field and a continuous evolution of the joint density-of-states (DOS) from 2D to 0D (delta-

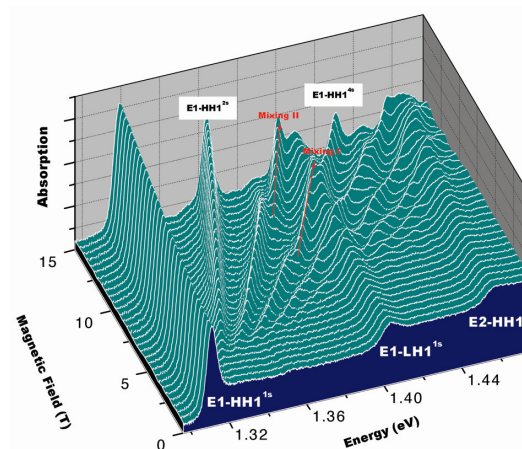


Figure 2. Magneto-absorption of 80 Å $\text{In}_{0.2}\text{Ga}_{0.8}\text{As}$ quantum wells, showing strong Landau quantization of the 1st heavy-hole states and mixing of the light-hole and heavy-hole states as the magnetic field increases. The density evolves from a 2D step-like profile at zero-field to a 0D delta-function character as the continuum states are suppressed.

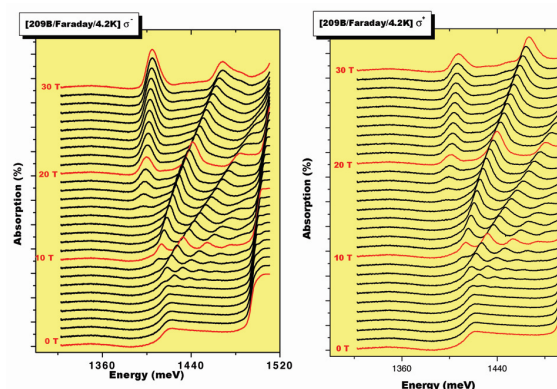


Figure 3. Magneto-absorption of n-doped $\text{In}_{0.2}\text{Ga}_{0.8}\text{As}$ quantum wells versus magnetic field for circularly polarized light. As the field increases above 15 T, a low energy state appears at 1400 meV below the heavy-hole exciton.

function) with increasing field (Figure 2). The formation of a new bound state (trion) in the n-doped sample, consisting of two electrons and a hole^{3,4} appearing at filling factors less than 2 and becoming highly polarized with decreasing filling factor (Figure 3). Our results agree with theoretical calculations based on $\mathbf{k}\cdot\mathbf{p}$ theory with interface strain.

Acknowledgements: This work is supported by NSF Materials Research Instrumentation grant DMR-0216838 and by the NHMFL In-House Research Program.

- 1 Yamamoto, Y., *et al.*, Mesoscopic Quantum Optics (John Wiley & Sons, New York, 1999).
- 2 Autler, S.H., *et al.*, *Phys. Rev.*, **100**, 703 (1955).
- 3 Stébé, B., *et al.*, *Superlattices Microstruct.*, **5**, 545 (1989).
- 4 Kheng, K., *et al.*, *Phys. Rev. Lett.*, **71**, 1752 (1993).

Magnetic Field Dependent Photoluminescence in Nitrogenated GaAsSb

Jones, E.D., Sandia National Laboratories
 Waldrup, K., Sandia National Laboratories
 Tozer, S.W., NHMFL
 Wei, X., NHMFL

The semiconductor alloy system, InGaAsN, is an important material for multi-junction solar cells with efficiencies greater than 40% and for 1eV-range laser systems. The introduction of small amounts of nitrogen (~2%) in the InGaAs alloy system greatly reduces the band gap energy, with reductions approaching 0.5 eV! This research program is thus aimed at understanding the fundamental nature of the effect of adding substitutional isoelectronic nitrogen atoms for arsenic. Our recent band structure calculations suggest that the reduction to the bandgap energy is a result of Γ -X and Γ -L mixing between the GaAs conduction band states. With this strong mixing, we also expected and found large mass changes, which is also in agreement with predictions based on the level mixing model. Because the effect of level mixing is a general phenomenon and not dependent upon the nature of GaAsN, it is important to demonstrate similar effects in other material systems. For this we have studied the effect of adding nitrogen (~1%) to GaAsSb strained quantum wells grown on GaAs substrates with GaAs barriers.

Figure 1 shows the dependence of the 1.3 K photoluminescence peak energy as a function of applied magnetic field for quantum wells with and without nitrogen. The bandgap energies for the GaAsSb and GaAsSbN strained quantum wells are respectively 1021 and 748 meV, which again demonstrates the bandgap reduction due to the presence of a small amount (1%) of nitrogen. The increase in mass can also be inferred from the data shown in Figure 1. At low magnetic fields, the diamagnetic shift can be approximated through first order perturbation theory and is proportional to $B^2\mu^{-3}$ where B is the magnetic field and μ is the exciton reduced mass. At high magnetic fields, the shift is proportional to $B\mu^{-1}$, but for intermediate fields the diamagnetic shift dependence upon field and excitonic reduced mass is rather complex. The exact value of the excitonic reduced mass must be extracted through modeling of the diamagnetic shift data to include the effects of strain. This work is in progress and no exact values are available to report at this time. A rough estimate, however, may be made from the slopes of the data, which suggest that the reduced mass of the exciton in the nitrogen-containing quantum well is about 2 to 4 times heavier than that of the non-nitrogenated, GaAsSb quantum well. If the material behaves as the InGaAsN

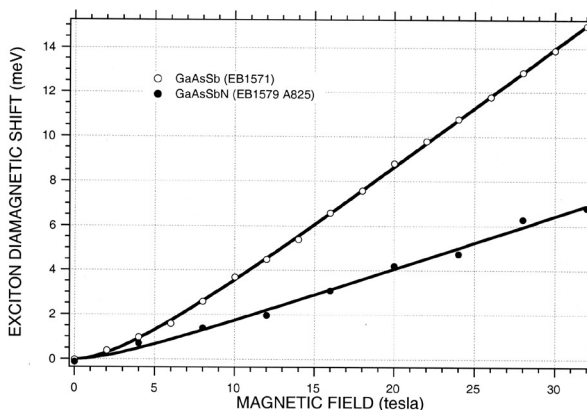


Figure 1. Magnetic field dependence of the exciton diamagnetic shift for GaAsSb (open circles) and GaAsSbN (filled circles) at 1.3 K

materials system, then the conduction-band mass makes the entire contribution to the increase in reduced mass of the exciton upon adding nitrogen to GaAsSb.

Optical Studies of Spin Polarized 2DEG in Modulation-Doped (Zn,Mn)Se/(Zn,Be)Se Quantum Wells in High Magnetic Fields

Keller, D., Physikalisches Institut der Universität Würzburg, Germany
 Astakhov, G.V., Physikalisches Institut der Universität Würzburg, Germany
 Yakovlev, D.R., Experimentelle Physik 2, Universität Dortmund, Germany
 Ossau, W., Physikalisches Institut der Universität Würzburg, Germany
 Barrick, T., NHMFL/LANL
 Crooker, S.A., NHMFL/LANL

The strong *sp-d* exchange interaction of the carriers with the localized Mn electrons in diluted magnetic semiconductors (DMSs) results in the well-known giant Zeeman splitting of the spin sublevels of the valence and conduction band. At present magneto-optical properties of undoped heterostructures (e.g. quantum well (QW) structures) based on wide-gap DMS are known in great detail, although only few investigations have been performed for the modulation-doped DMS quantum wells. ZnSe-based structures are particularly suitable for studies of Coulombic correlation effects in a 2DEG, due to the strong Coulombic interaction in ZnSe (exciton binding energy in bulk is 20 meV compared to 10 meV in CdTe).

In our experiments, we measured the photoluminescence and reflectivity spectra of modulation-doped $\text{Zn}_{0.995}\text{Mn}_{0.005}\text{Se}/\text{Zn}_{0.96}\text{Be}_{0.04}\text{Se}$ QWs with different electron densities. At zero magnetic field an increasing 2DEG density results in a broadening of the charged exciton line and a screening of the exciton line in the optical spectra. Figure 1 shows the energy shift of the transitions observed in PL (triangles) and reflectivity (squares) in magnetic field for $(\text{Zn,Mn})\text{Se}/(\text{Zn,Be})\text{Se}$ QW with electron density of $n_e = 3.2 \times 10^{11} \text{ cm}^{-2}$. The energy shift of the optical transitions in the undoped reference structure is shown by lines for comparison. Between 7 and 24 T new lines appear in the reflectivity spectra of the modulation doped sample, which can be attributed to combined exciton- (ExCR) and trion-cyclotron resonances (TrCR). These lines are due to the interaction of excitons and trions with free electrons on Landau

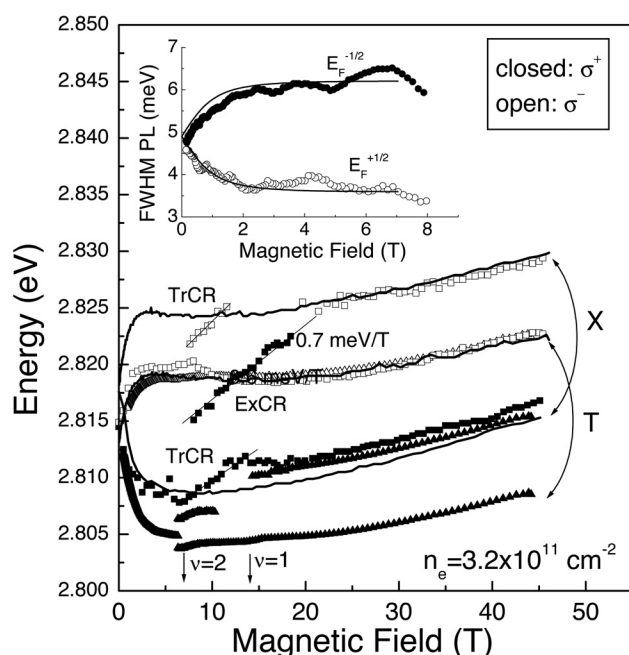


Figure 1. Energy position of the optical transitions in reflectivity (squares) and luminescence (triangles) spectra of a $\text{Zn}_{0.995}\text{Mn}_{0.005}\text{Se}/\text{Zn}_{0.96}\text{Be}_{0.04}\text{Se}$ QW with $n_e = 3.2 \times 10^{11} \text{ cm}^{-2}$. The exciton and trion energies for the undoped reference sample are shown by lines for comparison. The inset shows the full width at half maximum of the circularly polarized luminescence lines at low magnetic fields.

levels; for example, when the exciton is photogenerated in the vicinity of a background electron this electron can be excited from the lowest to higher Landau levels. The energy necessary for such an excitation is equal to the cyclotron energy of electrons. Simultaneous generation of exciton and excitation of a background electron provide a new state, which will give resonance in the reflectivity spectra. The electron density can be determined from the

characteristical changes of the optical spectra at integer filling factors.

A characteristic of DMS is the strong polarization of the 2DEG due to the giant Zeeman splitting. The inset in Figure 1 shows the full width at half maximum (FWHM) of the luminescence line of the modulation-doped sample. For the σ^+ polarization, the FWHM increases, while it decreases symmetrically in the σ^- polarization for small magnetic fields. We attribute this to the different occupation of the two electron spin levels, caused by the giant Zeeman splitting of the conduction band. The FWHM corresponds reasonably well with the Fermi energies $E_F^{+1/2}$ and $E_F^{-1/2}$ for electrons with spin $+1/2$ and $-1/2$. Lines show a simulation of the Fermi energies.

Results of this project are included in the following publications:

- 1 D. Keller, G.V. Astakhov, D.R. Yakovlev, T. Barrick, S.A. Crooker, L. Hansen, W. Ossau, and L.W. Molenkamp, Proc. 26th IC on the Physics of Semiconductors, Edinburgh, UK 2002, publication on CD.
- 2 D. Keller, G.V. Astakhov, D.R. Yakovlev, S.A. Crooker, L. Hansen, and W. Ossau, Proc. NATO workshop on Optical properties of 2D systems with interacting electrons, June 2002, St. Petersburg, Russia, NATO series book.

Acknowledgements: This work was supported in part by the Deutsche Forschungsgemeinschaft (SFB 410).

Cyclotron Resonance in Ferromagnetic III-V Semiconductors

Khodaparast, G.A., Rice Univ., Electrical and Computer Engineering

Kono, J., Rice Univ., Electrical and Computer Engineering

Sanders, G.D., UF, Physics

Sun, Y., UF, Physics

Stanton, C.J., UF, Physics

Munekata, H., Tokyo Institute of Technology

Wang, Y.J., NHMFL

The recent discovery of carrier-induced ferromagnetism in magnetic III-V semiconductors such as GaMnAs and InMnAs ¹⁻³ has not only opened up new device possibilities but also provided a novel system in which to study the physics of itinerant carriers interacting with localized spins. Various theoretical models have been proposed but the microscopic mechanism is still a matter of controversy. One of the open questions is the nature of the carriers mediating the exchange interaction between Mn ions, i.e., whether they reside in the impurity band (d-like), the delocalized valence bands (p-like), or some type of mixed states.

We are studying cyclotron resonance (CR) in ferromagnetic InMnAs/GaSb heterostructures. CR is a direct and accurate method for determining the effective masses (i.e., the curvature of the energy dispersion) of carriers and therefore the nature of the carrier states. Since these magnetic semiconductors usually have low carrier mobilities, a very high magnetic field is necessary to observe CR (i.e., $\omega_c \tau > 1$). We have observed CR in these systems, suggesting the existence of delocalized carriers. Shown in Figure 1 is a schematic band diagram of the samples studied. Due to the type-II band lineup plus the surface pinning of the Fermi energy, there are two hole “pockets,” one on the InMnAs side and the other on the GaSb side of the interface.

We initially observed hole CR in ferromagnetic InMnAs/GaSb heterostructures using destructive pulsed magnetic fields at the Megagauss Laboratory of the University of Tokyo.⁴ The observed CR spectra are strongly temperature-dependent, especially near and below the Curie temperature (T_c). Figure 2 shows typical CR data

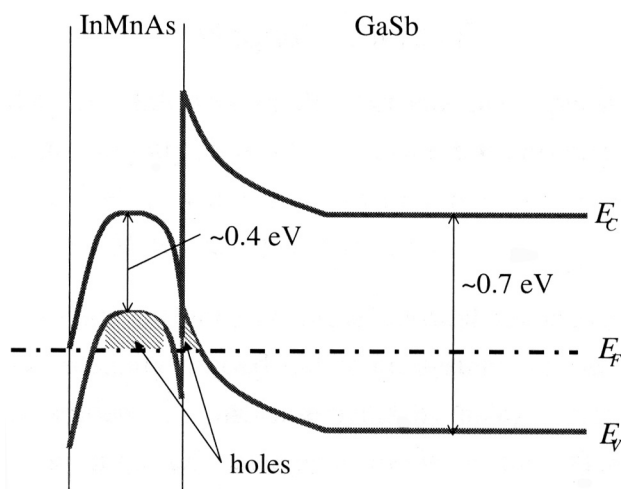


Figure 1. Schematic band diagram of the InMnAs/GaSb structures.

for two ferromagnetic samples taken with 10.6- μ m radiation. Here we observe two pronounced CR features with unusual temperature dependence. Feature A (~50 T) abruptly reduces its linewidth, shifts its resonance field, and increases its intensity at a temperature slightly above T_c . Feature B, which is absent at high temperatures, suddenly appears around T_c , rapidly grows in intensity with decreasing temperature, and becomes comparable to Feature A at low temperatures. To our knowledge, this is the first observation of CR in a ferromagnetic semiconductor.

In order to provide insight into these unusual features observed in ultrahigh pulsed fields, we have recently

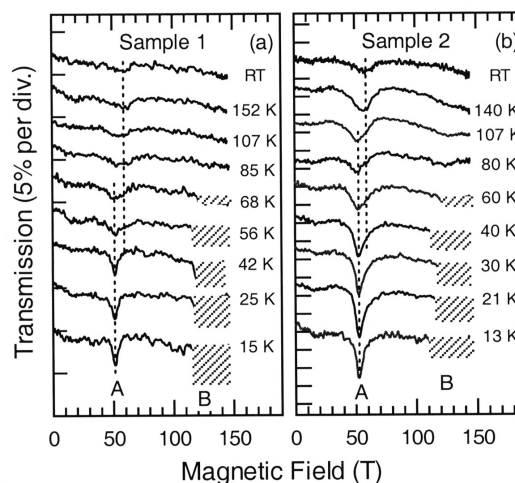


Figure 2. First CR data for InMnAs in the ferromagnetic phase. Feature A shows dramatic, sudden changes slightly above T_c and Feature B abruptly appears and grows at low temperatures. Data taken with hole-active circular polarized 10.6 μ m radiation. The T_c of the samples were 55 K and 30 K, respectively.

carried out more systematic and precise temperature- and photon-energy-dependent CR measurements by using Fourier transform infrared (FTIR) spectroscopy in high DC magnetic fields at the NHMFL in Tallahassee. Figures 3(a–c) show the transmission of far-infrared radiation through one of the ferromagnetic samples ($T_c = 35$ K) at $T = 4.2$ K as a function of photon energy at various magnetic fields from 17 T to 32 T. All traces are normalized to the zero-field transmission. Both Features A and B are clearly observed as dips, which increase with increasing field. Figure 4 summarizes the photon energy of the observed resonances versus magnetic field including data taken both

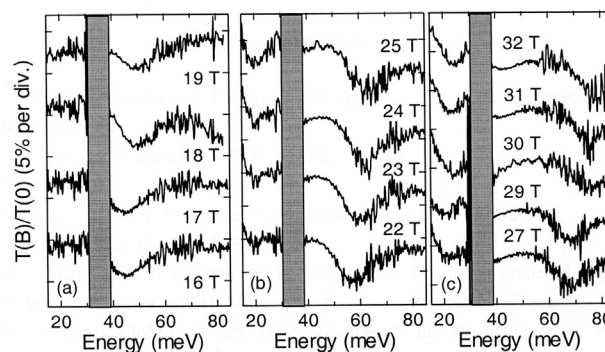


Figure 3. CR data for InMnAs in the ferromagnetic phase taken at various DC magnetic fields from 16 T to 32 T. Both Features A and B observed in pulsed measurements (see Figure 2) are present. The shaded area represents the reststrahlen band of the GaAs substrate, where transmission measurements are impossible.

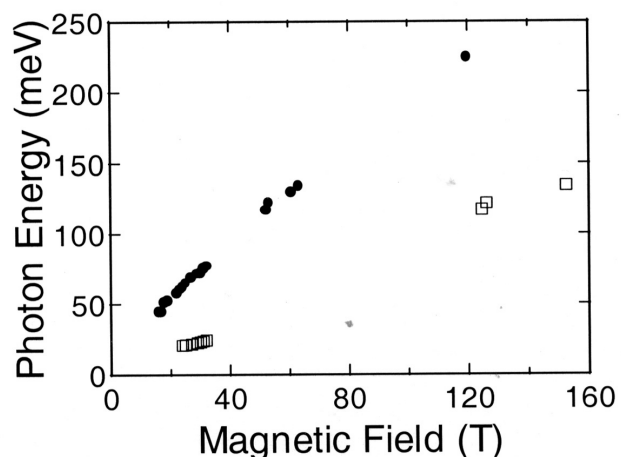


Figure 4. CR photon energy versus magnetic field for ferromagnetic InMnAs.

in the steady fields (up to 32 T) and in the pulsed fields (up to 150 T).

We are currently developing an 8-band **k-p** model to calculate hole Landau levels under the co-existence of a high magnetic field and ferromagnetic order. The comparison between the theoretical simulations and experimental data should provide significant new insight into the microscopic mechanism of carrier-induced ferromagnetism in ferromagnetic III-V semiconductors.

Acknowledgements: We gratefully acknowledge support from DARPA MDA972-00-1-0034 (SPINS), NSF DMR-0134058 (CAREER), and NEDO International Research Collaboration Program.

¹ Ohno, H., *et al.*, *Phys. Rev. Lett.*, **68**, 2664 (1992).

² Muneoka, H., *et al.*, *Appl. Phys. Lett.*, **63**, 2929 (1993).

³ Ohno, H., *et al.*, *Appl. Phys. Lett.*, **69**, 363 (1996).

⁴ Khodaparast, G.A., *et al.*, "Cyclotron Resonance of Itinerant Holes in Ferromagnetic InMnAs/GaSb Heterostructures," in: Proceedings of the 26th International Conference on the Physics of Semiconductors; see also cond-mat/0207485.

240 GHz EPR Studies of Intrinsic Defects in As-Grown 4H SiC

Kononov, V.V., Univ. of Alabama at Birmingham, Physics

240 GHz EPR measurements of as-grown nominally semi-insulating 4H SiC (Cree Inc.) detected two well separated centers, ID1 and ID2. The EPR parameters (g-values, HF constants) of ID1 and ID2 coincide with that of EI5 and EI6 centers previously detected in 2 MeV electron irradiated p-type 4H SiC:Al by 95 GHz EPR.¹⁻³ The defects in irradiated material were assigned to a positively charged carbon vacancy (EI5)² and silicon anti-site (EI6),³ respectively.

We report 240 GHz EPR studies of intrinsic defects in as-grown 4H SiC. Increased separation between the two centers at 240 GHz and the absence of additional spectral lines in as-grown SiC, which were presented in irradiated material, facilitated analysis of the defect structure. As the temperature decreased from 77 K to 4 K, with H//c-axis the g-value of ID1 remained constant at 2.00307, but the g-value of ID2 decreased from 2.00272 to 2.00235. Concomitantly, the intensity of ID1 decreased while that of ID2 increased. The ID1 and ID2 centers may be interpreted as two-carbon vacancy related defects. No evidence that the ID2/EI6 center represents a silicon anti-site was obtained. Illumination with NIR light quenched both ID1 and ID2 simultaneously, indicating close defect energy levels.

Acknowledgements: This work was supported by the Office of Naval Research.

¹ Son, N.T., *et al.*, *Mater. Sci. Forum*, **353-356**, 499 (2001).

² Son, N.T., *et al.*, *Phys. Rev. B*, **63**, 201201 (2001).

³ Son, N.T., *et al.*, *Phys. Rev. Lett.*, **87**, 45502 (2001).

Fractional Quantum Hall Effect in the Si/Si_{1-x}Ge_x Heterostructure

Lai, K., Princeton Univ., Electrical Engineering
Pan, W., Princeton Univ., Electrical Engineering
Tsui, D.C., Princeton Univ., Electrical Engineering
Xie, Y.H., Univ. of California at Los Angeles, Materials Science Engineering

The fractional quantum Hall effect (FQHE), which is a unique phenomenon of two-dimensional electron/hole systems in high magnetic field and low temperature, has been intensively studied during the past two decades. The high quality and lattice-matched nature of the GaAs/AlGaAs system makes it the best candidate material for such research. In recent years, there is great interest in the design and fabrication of new heterojunction material structures, for the realization of high mobility two-dimensional electron system (2DES) in strained Si. Comparing to the GaAs/AlGaAs system, its different band structure (e.g., valley degeneracy), as well as the large g-factor, are expected to introduce new degrees of freedom in the physics of strongly correlated 2DES in high magnetic field.

We report here the quantum transport results on the $\nu=2/3$ and $4/3$ FQHE states in the 2DES in the Si/Si_{0.75}Ge_{0.25} heterostructure at temperatures down to 40 mK and in B-field up to 42 T. Figure 1 shows the diagonal resistance R_{xx} and the Hall resistance R_{xy} . From the T-dependence of R_{xx} , an activation energy of ~ 0.6 K was deduced at $\nu=2/3$. It is small compared to the theoretically expected

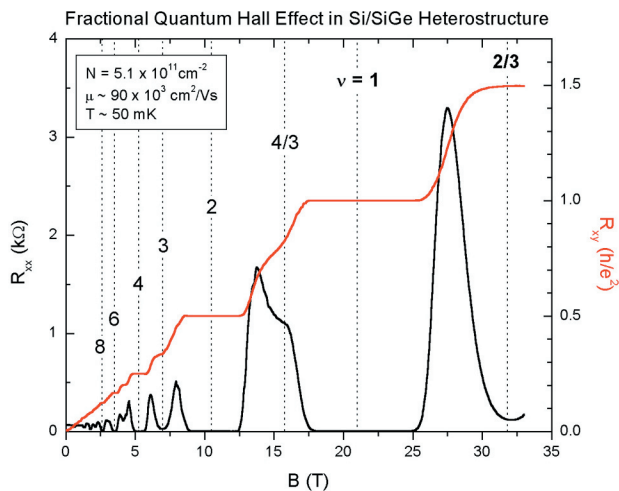


Figure 1. R_{xx} and R_{xy} in the Si/Si_{1-x}Ge_x heterostructure. Major filling factors are indicated.

value (~ 30 K) and to that measured in the GaAs/Al_xGa_{1-x}As heterostructures with similar electron scattering rate. This apparent discrepancy cannot be accounted for by finite thickness and Landau level mixing corrections, and remains to be explained. Tilting B-field experiments were performed to study the spin polarization of these two states. It is well documented that, in 2DES in GaAs/AlGaAs with increasing tilt angle (θ), the $\nu=2/3$ and $4/3$ states undergo a phase transition from a spin-singlet state to a spin-polarized state. Our tilting field data in the strained Si heterostructure, however, show that R_{xx} and R_{xy} maintain their strength up to the highest θ of 45° , from which we conclude that the $\nu=2/3$ and $4/3$ states are spin-polarized. This may be related to the Si electron valley degeneracy in this system.

Microwave Resonance of Wigner Crystal Phase Around Integer Quantum Hall Effect States

IHRP

Lewis, R.M., NHMFL/Princeton Univ., Electrical Engineering

Chen, Y., Princeton Univ., Electrical Engineering

Engel, L.W., NHMFL

Tsui, D.C., Princeton Univ., Electrical Engineering

Pfeiffer, L.N., Bell Laboratories, Lucent Technologies

West, K.W., Bell Laboratories, Lucent Technologies

We have observed microwave resonances in diagonal conductivity, $\text{Re}(\sigma_{xx})$ of high quality two dimensional electron systems in integer quantum Hall effect (IQHE) states. The resonances occur at Landau level filling factors

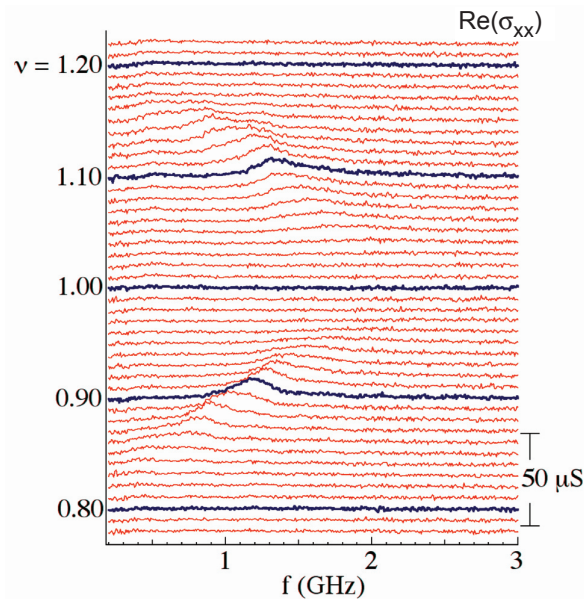


Figure 1. Spectra, $\text{Re}(\sigma_{xx})$ vs. frequency, f , for many Landau fillings ν , from 0.78 to 1.22. The bar on the right gives the $\text{Re}(\sigma_{xx})$ scale; spectra for successive fillings are offset proportional to ν .

$\nu=i+\nu^*$, for integer $i=1, 2, 3$ and 4 and small but nonzero $|\nu^*|$, for a sample of density $3 \times 10^{11} \text{ cm}^{-2}$ and mobility $2.4 \times 10^7 \text{ cm}^2/\text{V-s}$. Spectra taken around $i=1$ appear in the figure. The resonances are absent in a small range just around integer $\nu=i$, then develop as $|\nu^*|$ increases. The resonances become observable within the IQHE region of vanishing dc-limit $\text{Re}(\sigma_{xx})$, and hence appear to occur within the IQHE plateau. The resonances shift to lower frequency as $|\nu^*|$ increases, and disappear gradually at large enough $|\nu^*|$. They are suppressed on increasing the temperature above ~ 200 mK.

For ν near an integer value, the density of Landau quasiparticles (or quasiholes), is small so dilute quasiparticles (or quasiholes), can in principal form a Wigner crystal, which would be pinned by disorder. We interpret the resonances as pinning modes¹ of such “integer quantum Hall Wigner crystals,” analogous to the resonances seen in 2DES at the high magnetic field termination of a fractional quantum Hall effect series.² To our knowledge the present observations are the first evidence of Wigner crystallization playing a role in the IQHE.

¹ Fukuyama, H., *et al.*, *Phys. Rev. B*, **17**, 535 (1978).

² See, for example, Ye, P.D., *et al.*, *Phys. Rev. Lett.*, **89**, 176802 (2002).

Magnetoluminescence Study of MBE Grown p-Type GaSb:Mn Epilayers

Mallory, R., State Univ. of New York at Buffalo, Physics

Itskos, G., SUNY at Buffalo, Physics

Yasar, M., SUNY at Buffalo, Physics

Petrou, A., SUNY at Buffalo, Physics

Luo, H., SUNY at Buffalo, Physics

Wei, X., NHMFL

GaMnSb is one of the materials of interest for spintronics applications. In this report we present the results of a magnetoluminescence study of GaSb epilayers doped p-type with Mn acceptors. Even though the related GaAs:Mn system has been extensively investigated there has been very little work on GaSb:Mn. The samples used in this study were grown by molecular beam epitaxy on (100) GaAs substrates. Because of the large lattice mismatch between GaSb and GaAs, a 150 nm AlSb buffer layer was grown prior to the growth of the GaSb:Mn (thickness = 700 nm). The manganese concentration was controlled by the Mn cell temperature, set at 500 °C. The photoluminescence (PL) spectra were excited using the 514.5 nm line from an Argon-ion laser. The emitted light was analyzed by a spectrometer equipped with a liquid nitrogen cooled Germanium detector.

The spectra exhibit two features labeled “A” and “B” in Figure 1. Feature A (780 meV at $B = 0$) is identified as the conduction band to manganese acceptor (CB→Mn) transition. Feature B (760 meV at $B = 0$) is attributed to a (residual) donor to Mn acceptor transition. The identification is made on the basis of previous work by Georgitse *et al.*¹ and Fox *et al.*². The energy of feature A varies with magnetic field and has a slope of approximately 1 meV/T. Similar behavior has been observed for the corresponding CB→Mn transition in GaAs:Mn by Liu *et al.*³. The energy of feature B on the other hand does not change with magnetic field. No PL feature associated with the exciton (810 meV at $B = 0$) has been observed in these samples. We speculate that this is due to the fact that the exciting laser beam was not focused.

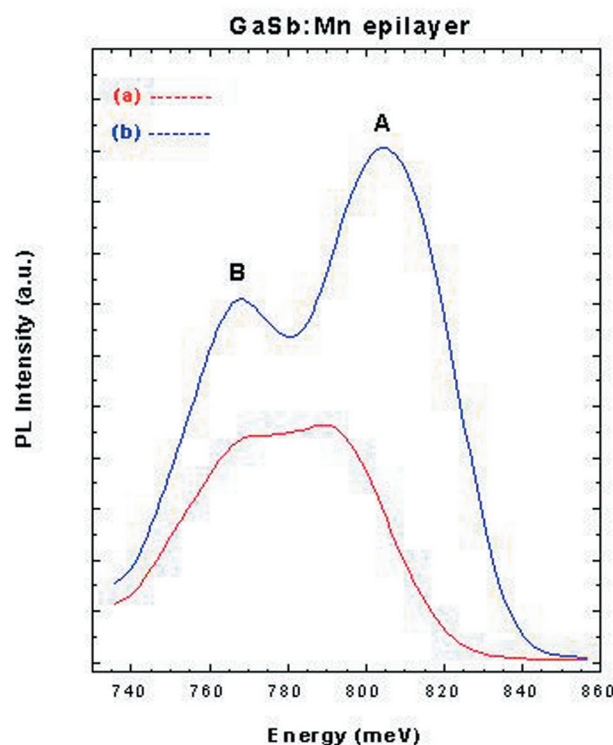


Figure 1. PL spectra from a GaSb:Mn epilayer at $T = 4$ K. (a) $B = 0$ (b) $B = 30$ T.

The objective of this preliminary study is to identify the CB→Mn transition in GaSb:Mn so that the circular polarization P of this feature can be studied as function of magnetic field. We expect steps in the P versus B plot similar to those observed in GaAs:Mn by Meining *et al.*⁴ from which the coupling constant between antiferromagnetically coupled Mn acceptors in GaSb can be determined.

Acknowledgements: This work was supported by DARPA/ONR N00014-00-1-0951.

¹ Georgitse, E.I., *et al.*, Sov. Phys. Semicond., **25**, 1219 (1991).

² Fox, A.M., *et al.*, Appl. Phys. Lett., **51**, 430 (1987).

³ Liu, X.C., *et al.*, 11th International Conference in High Magnetic Fields in Semiconductors, page 658 (World Scientific, Cambridge, Massachusetts, 1994).

⁴ Meining, *et al.*, 26th ICPS, Edinburgh UK, 2002, Conference Proceedings.

Magnetotunneling at Even-Denominator Fractions in an InAs-GaSb Tri-Layer System

Mendez, E.E., State Univ. of New York at Stony Brook,

Physics and Astronomy

Lin, Y., SUNY at Stony Brook, Physics and Astronomy

Magno, R., Naval Research Laboratory

Bennett, B.R., Naval Research Laboratory

We have observed minima at fractional Landau-level filling factors with even denominators in the high-field magnetotunneling conductance between two-dimensional gases formed in InAs-AlSb-GaSb heterostructures. A two-dimensional electron gas (2DEG), with density in the 5×10^{11} to $7 \times 10^{11} \text{ cm}^{-2}$ range, was formed at each InAs interface of the heterostructures, while a 2D hole gas was created in the central GaSb quantum well, typically 60 to 80 Å wide. At moderate fields, typically up to 7 T, the zero-bias conductance showed minima for integer Landau-level filling factors down to $\nu = 4$, consistent with 2D tunneling between non-interacting systems.¹ We have observed, however, that the high-field ($H \leq 33$ T) magnetoconductance deviates markedly from that behavior.

Our main findings are: (1) Minima corresponding to $\nu = 3, 2$, and 1 can be unusually weak and sometimes are even missing; (2) A minimum at (single layer) fractional filling factor $\nu = 5/2$ is easily observed in the highest-

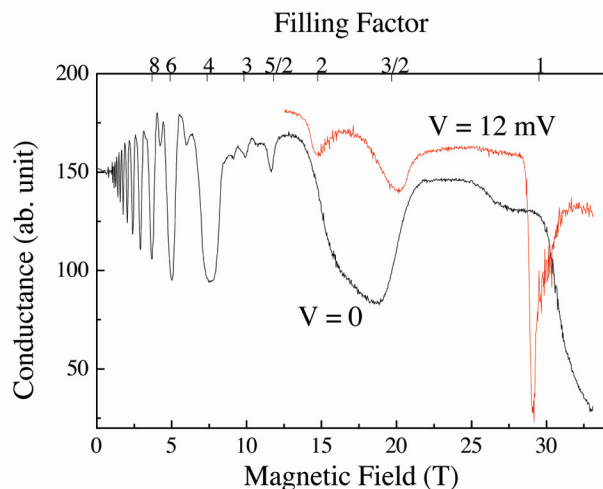


Figure 1. Magnetoconductance for an InAs-AlSb-GaSb-InAs heterostructure with an 80 Å GaSb region and 30 Å AlSb barriers. The field was normal to the layers; the temperature was 0.5 K. The trace from 0 to 33 T corresponds to the zero bias conductance, while that at high field only is for the case when a 12 mV bias is applied between the InAs electrodes. Although no minima at odd denominator fractions are discernible, minima for even denominators are apparent.

quality samples even at $T = 4$ K. (3) A small dc bias applied between the two end electrodes (partially) restores the missing minima at integer filling factors; (4) The temperature dependence of these anomalies is relatively weak in the $T = 4$ K to 0.5 K range. We attribute this behavior to the interplay between interlayer and intralayer interactions in the InAs/AlSb/GaSb/AlSb/InAs electron-hole tri-layer, analogous to that responsible for the richness of quantum-Hall phenomena in double-layer electron systems.

Acknowledgements: This work has been supported by the Army Research Office.

¹ González, E.M., *et al.*, *Phys. Rev. B*, **63**, 033308 (2001).

Electron-Electron and Electron-Phonon Interactions in Si/SiGe and CdTe/CdMgTe Probed Through Cyclotron Resonance

Miura, N., Univ. of Tokyo, Institute for Solid State Physics

Ikaide, T., Univ. of Tokyo, Institute for Solid State Physics

Ikeda, S., Univ. of Tokyo, Institute for Solid State Physics

Ostojic, G.N., Rice Univ., Electrical and Computer

Engineering

Zaric, S., Rice Univ., Physics and Astronomy

Kono, J., Rice Univ., Electrical and Computer Engineering

Shiraki, Y., Univ. of Tokyo, Applied Physics

Kuroda, S., Univ. of Tsukuba, Institute of Material Science

Takita, K., Univ. of Tsukuba, Institute of Material Science

Wang, Y.J., NHMFL

The effect of electron-electron interactions on the cyclotron resonance of 2-dimensional systems is an intriguing problem that has attracted much attention. Despite Kohn's theorem, which states that the effect of the electron interactions should be invisible in cyclotron resonance,¹ many experimental results have been reported on novel phenomena caused by electron-electron interactions in cyclotron resonance.^{2,3} They can show up if there are two different kinds of carriers (such as electrons with different spins, or in different valleys) or if the translational symmetry is broken in the system. Recently, we have observed the mode coupling between the spin-up states and spin-down states in the cyclotron resonance in InAs/AlSb quantum wells under very high magnetic fields.⁴ The relative intensity of the spin-split cyclotron resonance showed a peculiar dependence on the temperature, which was attributed to the electron-electron coupling. Another example of the electron-electron interaction is the oscillation of the effective mass and the

line-width depending on the filling factor of the Landau levels. The phenomena have been observed in GaAs/AlAs and CdTe/CdMgTe heterostructures. They are attributed to the impurity potentials that are screened by carriers. In recent experiments we have observed prominent mass and linewidth oscillations with filling factor.

Here, using the DC facility at the NHMFL in Tallahassee, we have observed unusual field-dependent cyclotron masses in a Si/SiGe quantum well (Figure 1) and a CdTe/CdMgTe quantum well (Figure 2) in high magnetic fields

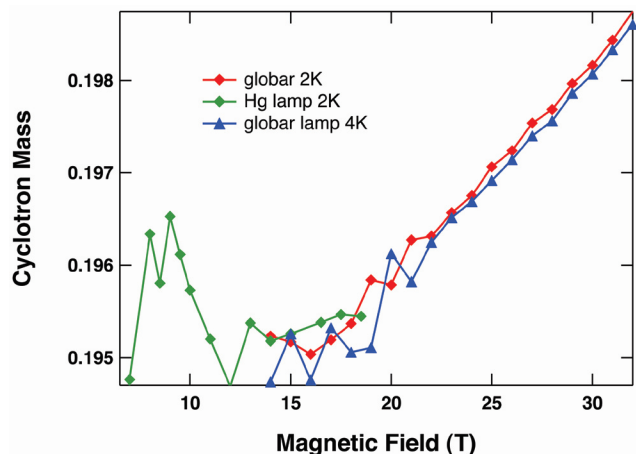


Figure 1. Cyclotron mass in Si/SiGe quantum well.

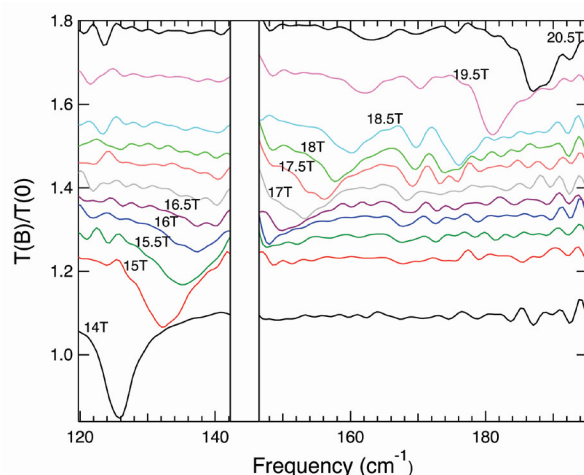


Figure 2. Cyclotron mass in CdTe/CdMgTe quantum well.

up to 33 T. In a high mobility Si/SiGe quantum well sample (well-thickness = 10 nm, $n = 2.0 \times 10^{11} \text{ cm}^{-2}$, $\mu = 5.0 \times 10^4 \text{ cm}^2/\text{Vs}$ at 20 K), a sharp cyclotron resonance peak was observed, having effective masses between $0.191 m_0$ and $0.194 m_0$, depending on the filling factor. The effective mass shows a maximum at a filling factor $\nu = 1$ ($B = 8.3 \text{ T}$) followed by an almost linear increase at

higher fields above 15 T. The mass increase between 15 T and 30 T reached 1.6 %, which is much larger than what is expected from band non-parabolicity, suggesting the importance of electron-electron interactions. In a CdTe/CdMgTe quantum well (well-thickness $\sim 10 \text{ nm}$, $n = 6.8 \times 10^{11} \text{ cm}^{-2}$), a large polaron pinning effect was observed near the LO phonon energy. In the gap between the two modes due to the anti-crossing, two absorption lines were observed.

¹ Kohn, W., *Phys. Rev.*, **123**, 1242 (1961).

² Summers, G.M., *et al.*, *Phys. Rev. Lett.*, **70**, 2150 (1993).

³ Engelhardt, C.M., *et al.*, *Surf. Sci.*, **305**, 23 (1994).

⁴ Arimoto, H., *et al.*, *Proc. 9th Int. Conf. Narrow Gap Semiconductors* (Berlin, 1999), eds. Puhlman, N., *et al.*, p. 10-15 (Humboldt University, 2000).

Quantum Hall Ferromagnetism in InSb Heterostructures

Murphy, S.Q., Univ. of Oklahoma, Physics and Astronomy
Chokomakoua, J.C., Univ. of Oklahoma, Physics and Astronomy

Santos, M.B., Univ. of Oklahoma, Physics and Astronomy

During a very successful run at the NHMFL in September 2002 we were able to observe quantum Hall ferromagnetism (QHF) in InSb heterostructures. QHF is an exotic form of ferromagnetism which, like standard ferromagnetism, results from the ordering of a quantum number. In the case of QHF the ordering is not restricted to electronic spin, but can also include combinations of spin and orbital angular momentum called pseudospin. QHF can be observed in a two-dimensional system in which single particle energy levels are forced to cross. At the point of degeneracy, many body interactions conspire to maintain a single ground state that can be either of the degenerate single particle states or a linear combination. The system is said to pseudospin polarize with all the electrons close to the Fermi level in a common state. Like more standard ferromagnetism, QHF has different classes including easy plane (XY) and easy-axis (Ising), complete with hysteresis.

In our case the single particle levels were associated with spin and orbital degrees of freedom. While the electron spin (Zeeman energy) is sensitive to all components of the magnetic field, the orbital motion (cyclotron energy) is sensitive only to the perpendicular component; hence we were able to induce QHF in InSb heterostructures by use of a tilted magnetic field. InSb is a good choice of material for such experiments as it has a large ratio of Zeeman to cyclotron energy even in the absence of a tilted field. The signature of a QHF state is a quantum Hall state that does not disappear at any angle. Key to the quantum Hall effect is a gap between single particle energy states. At

the tilt angle corresponding to degeneracy in the absence of exchange interactions, the quantum Hall effect would disappear when the gap between single particle states disappears. Exchange interactions in a QHF, however, would preserve the gap and sustain a quantum Hall effect.

In Figure 1, taken at a fixed tilt angle, one can see a strong QH state at filling factor 2 at low temperature. This QH state does not disappear at any angle. Curiously, however, a large resistance peak grows in the middle of the QH minimum at filling factor 2 as the temperature is raised.

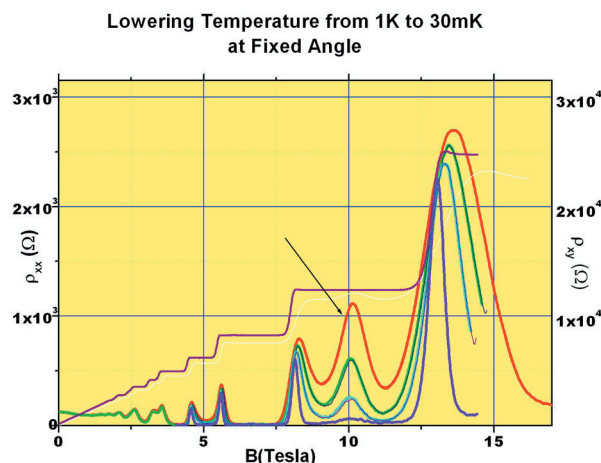


Figure 1. The longitudinal resistance of an InSb quantum well is shown at different temperatures. The strong QH state at filling factor 2 is present at all tilt angles indicating quantum Hall ferromagnetism. As the temperature is increased from 30 mK to 1 K, a large resistance peak grows from the quantum Hall minimum. This peak can be explained as dissipative electron transport along quantum Hall ferromagnetic grain boundaries. Also shown in the figure is the Hall resistance displaying strong plateaus.

Longitudinal Resistance Behavior as a function of Tilt Angle at 1K

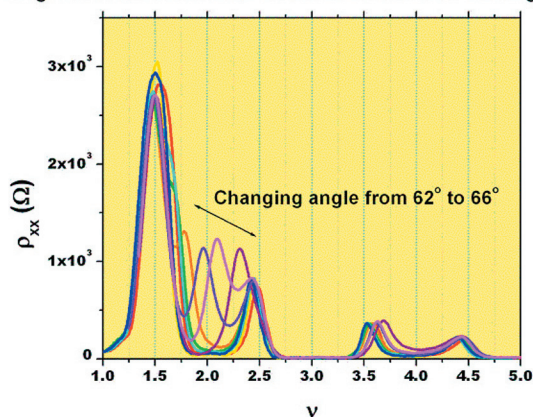


Figure 2. The resistance peak at 1 K can be moved through the minimum at filling factor 2 as the angle is changed.

This feature is interpreted as resulting from dissipative electronic transport at grain boundaries separating QHF states with different orientations. Figure 2 shows that the additional peak can be shifted by sweeping the tilt angle. This shift is consistent with theoretical predictions for the behavior of QHF.

Acknowledgements: This research was supported by NSF-0209371, NSF-9733949, and the OU-AU MRSEC.

Temperature Dependence and Mechanism of Electrically Detected ESR at the $\nu=1$ Filling Factor of a Two-Dimensional Electron System in GaAs Quantum Wells

Olshanetsky, E., UF, Physics

Pilla, M., UF, Physics

Caldwell, J.D., UF, Chemistry

Liu, S.-c., UF, Physics

Bowers, C.R., NHMFL/UF, Chemistry

Electrically detected electron spin resonance (EDES) signals were acquired as a function of temperature in the 0.3 K to 4.2 K temperature range in an AlGaAs/GaAs multiple quantum well sample at the $\nu=1$ filling factor at 5.7 T. In the particular sample studied, the line width is approximately temperature independent, while the amplitude exhibits a maximum at about 2.2 K and vanishes with increased or decreased temperature. To explain this observation, the temperature dependence of the signal amplitude was calculated assuming a heating model. The model ascribes the resonant absorption of microwave power of the 2DES to the uniform mode of the electron spin magnetization where the elementary spin excitations at filling factor $\nu=1$ are taken to be spin waves, while the short wavelength spin wave modes serve as a heat sink for the absorbed energy. Due to the finite thermal conductance to the surroundings, the temperature of the 2DES spin wave system is increased, resulting in a thermal activation of the longitudinal magnetoconductance. The proposed heating model correctly predicts the location of the maximum in the experimentally observed temperature dependence of the EDES amplitude. It also correctly predicts that the signal should vanish as the temperature is increased or decreased. The results of the present study demonstrate how experimental EDES studies can, under appropriate conditions, provide data that can be used to discriminate between competing theories for the magnetic ordering and magnetic excitations of a 2DES in the regime of the quantum Hall effect.

Fractional Quantum Hall Effect of Composite Fermions

Pan, W., Princeton Univ., Electrical Engineering/NHMFL
Störmer, H.L., Columbia Univ., Physics and Applied

Physics/Bell Labs, Lucent Technologies

Tsui, D.C., Princeton Univ., Electrical Engineering

Pfeiffer, L.N., Bell Labs, Lucent Technologies

Baldwin, K.W., Bell Labs, Lucent Technologies

West, K.W., Bell Labs, Lucent Technologies

The composite fermion (CF) model has been very successful in providing a rationale for constructing the principle FQHE sequences around major even-denominator fractions, such as $\nu=p/(2p\pm1)$ around $\nu=1/2$ and $\nu=p/(4p\pm1)$ around $\nu=1/4$, where $p = 1, 2, 3$, etc. According to this model, the e-e interaction is absorbed very effectively by forming a many-body particle, the CF, by means of the attachment of quantized vortices. As a result, the residual interaction between CFs is virtually zero or very weak and CFs can be treated as independent particles. On the other hand, the applicability of the CF model to the higher order FQHE states, where the residual interaction between CFs may be important, has not been tested experimentally, largely due to the extreme fragility of these states. Such experimental tests are very desirable, since only they can tell us if and how the CF model extends beyond the simple even-denominator fractions and its descendants to more complex fractions and, eventually, to all rational fractions. With the advent of yet higher-quality two-dimensional electron systems exploration of some of these fractional states has become feasible.

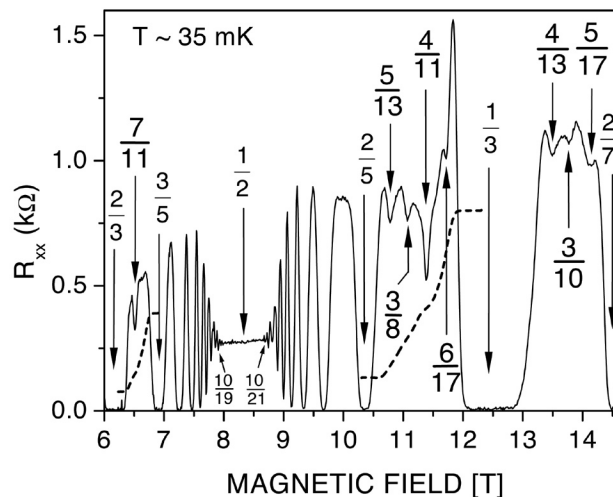


Figure 1. R_{xx} in the regime of $2/3 > \nu > 2/7$. Dashed traces are the Hall resistance R_{xy} around $\nu=7/11$ and $\nu=4/11$.

In a very clean specimen we observed new fractional states at $\nu=4/11, 5/13, 6/17$ between $\nu=2/5$ and $\nu=1/3$, as well as the $\nu=4/13$ and $5/17$ states between $\nu=1/3$ and $\nu=2/7$. A weak R_{xx} minimum was even observed at $\nu=4/19$ between $\nu=2/9$ and $\nu=1/5$. The newly found fractions do not belong to any principle FQHE sequences around $\nu=1/2$ or $\nu=1/4$ and they do not fit into the standard series of integral quantum Hall effects of composite fermions. One intuitive way to understand these new fractions is to interpret them as the FQHE states of CFs. In this sense, they are the FQHE states in the first Landau level of CFs. It is very interesting to note that a self-similarity seems to be at work for the patterns of FQHE features of electrons and CFs, e.g., the relative strength of FQHE states of CFs resembles the relative strength of electron FQHE, and the progression of their discovery.

At this stage, the physical origin of the FQHE states of CFs is unsolved. Yet, their existence clearly points to the importance of residual interaction between CFs.

Transition from an Electron Solid to the Sequence of Fractional Quantum Hall States at Very Low Landau Level Filling Factor

Pan, W., Princeton Univ., Electrical Engineering/NHMFL
Störmer, H.L., Columbia Univ., Physics and Applied

Physics/Bell Labs, Lucent Technologies

Tsui, D.C., Princeton Univ., Electrical Engineering

Pfeiffer, L.N., Bell Labs, Lucent Technologies

Baldwin, K.W., Bell Labs, Lucent Technologies

West, K.W., Bell Labs, Lucent Technologies

The ground state of a two-dimensional electron system (2DES) in the presence of a high magnetic (B) field is the result of a competition between electrostatics and subtle quantum mechanics, leading to intricate electron-electron correlations. At extremely high magnetic field and low carrier concentration electrons are forced into orbits that are tiny compared to their separation. As a consequence mutual wave function overlap vanishes, electrostatics dominates, and an electron crystal—analogue to a classical Wigner crystal of point charges—is expected to form. On the other hand, with decreasing magnetic field, a transition from the Wigner crystal phase to the FQHE liquids is expected to occur around $\nu \sim 1/7$.

Recently, we performed systematic electronic transport studies on an ultra-high mobility 2DES in a wide GaAs/AlGaAs quantum well and observe local minima in R_{xx} at multiple low Landau level filling factors $\nu=2/11, 3/17, 3/19, 2/13, 1/7, 2/15, 2/17$, and $1/9$. These minima represent a clear signature of a developing FQHE state and are

equivalent to $\nu = p/(6p \pm 1)$, $p = 1, 2$, and 3 , around $\nu = 1/6$, and $\nu = 1/(8p \pm 1)$, $p = 1, 2$, around $\nu = 1/8$. The FQHE states reside on top of a large background, which develops for filling factors lower than $\nu \sim 1/5$. Each of these developing FQHE states appears only above a filling factor-specific temperature, which lies between ~ 100 mK and ~ 300 mK. The observed behavior is well accounted for by melting of the Wigner crystal phase, expected to exist at such low filling factors, into the series of FQHE liquids.

It is interesting to note that the observed FQHE sequence follows the series of composite fermion (CF) Landau levels expected to emanate from a CF liquid at $\nu = 1/6$ and $\nu = 1/8$. This demonstrates the continued applicability of the CF model for the FQHE states well into the Wigner crystal regime.

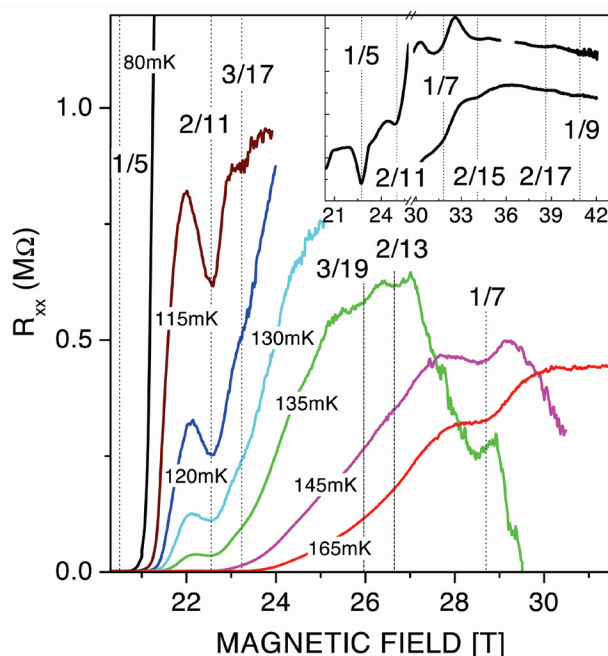


Figure 1. R_{xx} above 20 T at various temperatures. The vertical, dashed lines show the positions of the Landau level filling factors $\nu = 1/5, 2/11, 3/17, 3/19, 2/13, 1/7, 2/15, 2/17$, and $1/9$.

Toward Spectroscopy of Single Colloidal Quantum Dots in Low Temperatures and High Magnetic Fields

Preiner, M.P., Stanford Univ., Applied Physics

Hollingsworth, J., LANL

Petruska, M., LANL

Klimov, V.I., LANL

Crooker, S.A., NHMFL/LANL

The properties of semiconductor quantum dots in external magnetic fields are currently of great interest, due to their unique optical properties and possible uses for spintronics applications. There remain unanswered questions, however, about their electronic and magnetic structures, particularly in colloidal nanocrystalline quantum dot (QD) systems that constitute promising building blocks for the bottom-up assembly of macroscopic “artificial materials” having engineered functionality. In particular, some of the most powerful techniques for investigating quantum dot systems, such as single molecule spectroscopy, are difficult in high magnetic fields due to the size and access constraints imposed by high-field magnets.

Typical single molecule spectroscopy systems use high power microscope objectives, precision XYZ positioners, and sensitive CCD detectors to isolate and view single molecules. These conventional systems, however, are much too large to fit into the cryogenic bores of typical high-field magnets. In this work we have demonstrated the feasibility of a system that allows us to perform single molecule spectroscopy in high magnetic fields, opening up the possibility of measuring important QD properties such as the g-factor and Zeeman splitting of the band-edge exciton states. The system is remarkably simple and compact, and with it we have been able to observe many of the characteristic properties of single QDs, such as blinking, bleaching, spectral diffusion, and even single phonon-replica peaks.

The spectroscopic system uses a single-mode optical fiber to both excite and collect the emitted fluorescence from the QDs. By dipping one end of the fiber into a sufficiently dilute solution of QDs, we create a film that contains only a few optically active dots over the small 3-5 micron diameter of the fiber core. We can then place the fiber into a cryostat and/or high field magnet while coupling the other end into a CCD spectrometer. The extremely narrow linewidths of CdSe QDs at low temperatures allows us to distinguish individual dots on the fiber tip, so that multiple dots may be viewed at the same time. Figure 1 shows the narrow emission spectra from a single dot located on

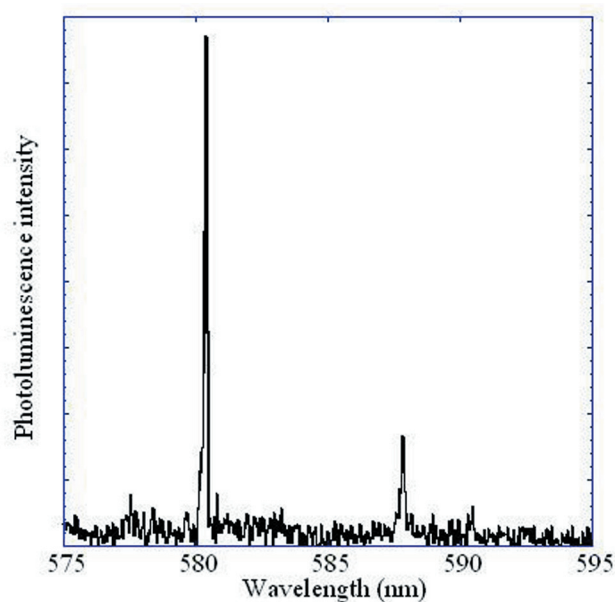


Figure 1. Narrow emission spectra from a single quantum dot located on the tip of a single-mode optical fiber at 4 K. The main emission peak is clearly seen, as well as a smaller phonon replica ~25 meV lower in energy. Exposure time was 20 seconds.

the tip of the singlemode fiber at 4 K. Phonon-assisted recombination is also evident by the phonon replica ~25 meV lower in energy.

Transport in Low Dimensional Niobium Oxychlorides Compounds

Qualls, J.S., Wake Forest Univ., Physics*

Peng, L., Wake Forest Univ., Physics

Lachgar, A., Wake Forest Univ., Chemistry

Extended solids containing transition metal clusters have attracted significant interest in applied and fundamental materials research due to their remarkable physical and structural properties.¹ A number of niobium oxychlorides compounds have been synthesized at Wake Forest University. These low-dimensional and open-framework materials (containing octahedral metal clusters) must be characterized to reach a fundamental understanding of the correlation between the cluster configuration and the framework dimensionality. By using a combination of ligands to make compounds with new structure types, and perhaps interesting magnetic or conductivity properties, this work will aid in identifying and understanding the structure determining factors that will ultimately lead to making these materials by design. This approach has already led to the successful synthesis of novel compounds with 3D, 2D, and 1D framework that need to be characterized and investigated. This work involved looking

at six such compounds, $[\text{Nb}_2(\text{en})_6]\text{Cl}_2$, $\text{In}_x\text{Nb}_6\text{Cl}_{12}\text{O}_2$, $\text{Cs}_2\text{Ti}_2\text{Nb}_6\text{Cl}_{14}\text{O}_5$, $\text{Rb}_{1.7}\text{TiNb}_6\text{Cl}_{14.7}\text{O}$, $[(t\text{-Bu}_4\text{N})_3\text{Nb}_6\text{Cl}_{18}]$, and $\text{Ti}_2\text{VNb}_6\text{Cl}_{17}\text{O}$. Band structure calculations done by an extended Hückel tight-binding method predicted that these compounds would display metallic properties.

For all compounds the electrical resistivity was measured in the temperature range 4.2 K to 300 K. Samples were irregular cubic shaped single crystals with sides around 20~30 μm . Leads were attached using carbon XC-12 conductive paint. The electrical resistivity of all

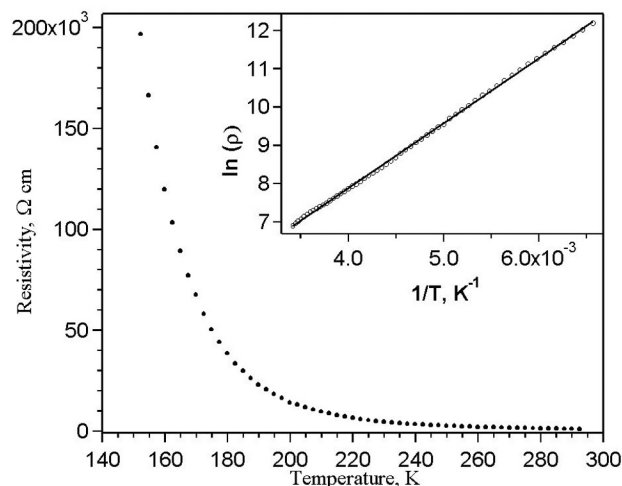


Figure 1. Electrical resistivity of $\text{Ti}_2\text{VNb}_6\text{Cl}_{17}\text{O}$ as a function of temperature. Insert: logarithm of electrical resistivity as a function of $1/T$. The resistivity at room temperature is $9.92 \times 10^2 \Omega\text{-cm}$. The thermal activation energy for the conduction estimated from the linear fit of the plot of $\ln \rho$ vs. $1/T$ in the temperature range 150 to 300 K is 0.29 eV.

compounds increased exponentially with decreasing temperature (see Figure 1), indicating a semiconducting behavior. The results were in conflict with the expected metallic behavior. It is possible that the materials may be metallic and undergo a metal-insulator transition due to magnetic interactions or low dimensional electronic instabilities. Further measurements, however, are needed to clarify this possibility.

High field magnetization studies using a torque magnetometer in conjunction with a general radio capacitance bridge were then performed. Unfortunately small sample size and weak magnetization signals did not allow for the magnetic properties to be clearly resolved. Larger samples or powders will be required before further investigation of these compounds can be made.

* Current address: University of Texas Pan American

¹ Simon, A. in Schmidt, G. (ed.), Clusters and Colloids - From Theory to Applications; VCH Publishers: Weinheim, (1994).

Magnetoplasmon Resonance of an AlGaAs/GaAs 2DEG at 50 mK

Shaner, E.A., Princeton Univ., Electrical Engineering
 Lyon, S.A., Princeton Univ., Electrical Engineering
 Engel, L., NHMFL
 Wei, X., NHMFL

We observed magnetoplasmon/cyclotron resonance up to 1.2 T (about 500 GHz) in an AlGaAs/GaAs 2DEG sample by launching short (1.8 ps) electrical pulses on a coplanar waveguide (CPW) that was capacitively coupled to the 2DEG. By time resolving pulse propagation on the guide, we are able to see the effect of dipolar resonances in the 2DEG. A summary of the time resolved results is displayed in Figure 1. The previous best (which we published¹) was about 0.5 T (200 GHz). We have shown that we can operate our devices at dilution refrigerator temperatures in magnetic fields up to 18 T. Future experiments will involve including DC transport devices on the chip to provide temperature and field information.

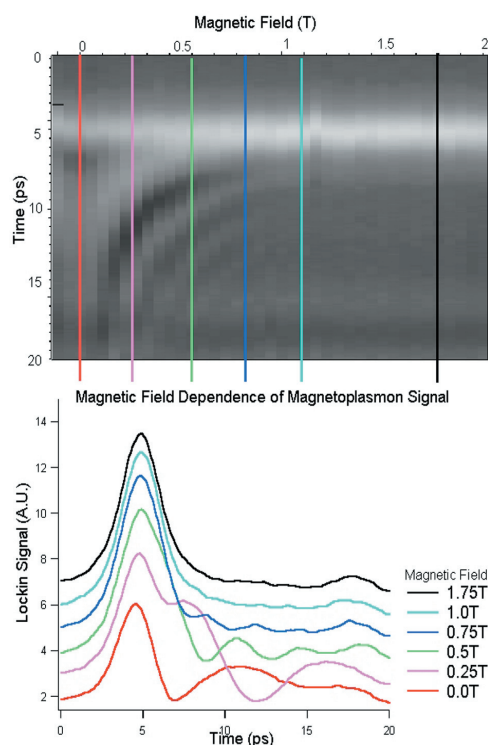


Figure 1. Time resolved pulse propagation plotted at various magnetic fields. The top image is a compilation of scans taken at NHMFL at 50 mK bath temperature. Line scans across the image are plotted separately in the graph below for further clarity. As magnetic field is increased, the ringing trailing the initial excitation pulse is seen to change frequency. This is due to the cyclotron component of the magnetoplasmon resonance.

¹ Shaner, E.A., *et al.*, *Phys. Rev. B*, **66**, 041402(R) (2002).

Cyclotron Resonance of Two-Dimensional Electrons in Nitride Heterostructures

Syed, S., Columbia Univ., Physics
 Manfra, M.J., Bell Laboratories
 Wang, Y.J., NHMFL
 Störmer, H.L., Columbia Univ., Physics, and Bell Laboratories
 Pfeiffer, L.N., Bell Laboratories
 Molnar, R.J., Massachusetts Institute of Technology, Lincoln Laboratory

We have conducted extensive cyclotron resonance (CR) studies on two-dimensional electron systems (2DES) at the interface of AlGaN and GaN. Samples used in this study consist of 20 μm thick GaN grown on the [0001] face of sapphire by hydride vapor phase epitaxy (HVPE), followed by 40 to 500nm of GaN deposited by molecular beam epitaxy (MBE). The GaN layers are capped by ~ 30 nm of AlGaN. The density of electrons at the heterointerfaces was varied by changing the concentration of Al in the capping layer. We investigated samples with densities ranging from 1 to $5 \times 10^{12} \text{ cm}^{-2}$ and carrier mobilities between 17,000 and 40,000 $\text{cm}^2 / \text{Vsec}$.

Our interests were two-fold: to understand the primary scattering mechanisms for electrons in the two-dimensional layer and to determine the non-parabolicity of the conduction band of the host material by measuring electron effective mass. In a CR experiment, the effective mass of the excited carriers can be determined from the resonance absorption energy and the lifetime, τ_{CR} , of the inter-Landau level transitions can be measured from the line width of the absorption line.

In order to get a complete picture of scattering at low temperatures, we also determined the transport lifetime, τ_c , from the mobility and the quantum lifetimes, τ_q , from magnetoresistance. While τ_q is a measure of all scattering events, τ_c measures the time for backscattering, which can involve several events in the case of small angle scatterings. Comparing the cyclotron lifetime with quantum lifetime reveals $\tau_{\text{CR}} \gg 6\tau_q$ over the entire density range investigated. Our modeling of magnetoresistance data suggests that τ_q is strongly affected by density inhomogeneities, making deductions of τ_q in our specimens very unreliable. We conclude that τ_{CR} is a better measure of all scattering events in our nitride systems. Moreover, by determining the ratio $\tau_c / \tau_{\text{CR}}$ for various densities, we derive that in the range $1 - 4 \times 10^{12} \text{ cm}^{-2}$ scattering becomes increasingly small angle with increasing densities.

As for the mass measurements, we compare our data to a simple two-band model of non-parabolicity. We observe that such a simple model cannot account for the non-parabolicity of the conduction band and that at least a 5-band k.p calculation is required. For the wurtzite GaN such a calculation has not yet been performed.

Fractional Quantum Effect Studies at the AlGa_xN/GaN Interface

Syed, S., Columbia Univ., Physics

Manfra, M.J., Bell Laboratories

Gervais, G., NHMFL

Störmer, H.L., Columbia Univ., Physics and Applied Physics, and Bell Laboratories

Pfeiffer, L.N., Bell Laboratories

Molnar, R.J., Massachusetts Institute of Technology, Lincoln Laboratory

We have conducted electrical transport experiments on two-dimensional electron systems (2DES) at the interface of Al_xGa_{1-x}N and GaN. The samples are grown using a combination of hydride vapor phase epitaxy (HVPE) and molecular beam epitaxy (MBE) on sapphire substrates. The HVPE templates are 20 μm thick and are doped with Zn to compensate for parasitic carriers that are created unintentionally during the growth process. The 2DES's in these heterostructures reside at the interface between a typically 400 to 500 nm thick, MBE-grown GaN layer, and the top AlGa_xN of typically 30 nm thickness. A range of 2D electron density is achieved by systematically controlling the Al% in the Al_xGa_{1-x}N of each sample. The mobilities of our samples are between 20,000 and 30,000 cm²/Vsec making them the best nitride heterostructures currently available.

Our experiments were done on samples with densities between 0.95 and 1.2 × 10¹² cm⁻² in up to 40 T field, using Ti/Al contacts evaporated around the edges of the samples. Both longitudinal magnetoresistance and Hall measurements were conducted at temperatures ranging from 40 mK up to 300 mK using 10 nA excitation current. The samples showed clear evidence of the integer quantized Hall effect (IQHE) including vanishing magnetoresistance and quantized Hall plateaus. In fields above 30 T, we were able to observe for the first time the spin resolved ν=1 state in a GaN/AlGa_xN specimen. Beyond the IQHE we found clear evidence for the existence of the ν=5/3 fractional states between 23 T and 30 T using the upper part of the temperature range available. Activation energy measurements showed that the ν=5/3 state in our samples is rather insensitive to temperature changes. This points to a high level of residual potential fluctuations, which localize a sufficient fraction

of carriers to mask a clear observation of the FQHE and a measurement of its activation energy gap.

Acknowledgements: We would like to thank Tim Murphy and Eric Palm for their technical help.

Effective Mass of a GaAs Two-Dimensional Electron System in Parallel Magnetic Field

Tutuc, E., Princeton Univ., Physics

Melinte, S., Princeton Univ., Electrical Engineering

De Poortere, E.P., Princeton Univ., Electrical Engineering

Shayegan, M., Princeton Univ., Electrical Engineering

The spin-polarization of a dilute two-dimensional electron system (2DES) is a topic of current interest as it may shed light on the controversial problem of metal-insulator transition in 2D.¹ A technique commonly used to study the spin polarization of 2DESs is to measure its response to a tilted or parallel magnetic field (*B*). In such experiments it is generally assumed that the parallel component of the magnetic field couples only to the spin degree of freedom of the 2DES.^{2,3,4} A more subtle, and often overlooked, effect is the deformation of the Fermi surface due to the combination of parallel *B* and of the 2DES finite layer thickness.⁵ The deformation of the Fermi surface can induce an enhancement of the band effective mass,⁶ *m*^{*}, which may affect the degree of spin polarization in a parallel *B*.

Following recent measurements of spin polarization in modulation-doped GaAs 2D hole³ and electron⁴ systems, we carried out experiments to determine *m*^{*} vs. applied parallel *B*. We used a GaAs 2DES sample with an as-grown density of 4.2 × 10¹⁰ cm⁻² and a mobility of 400,000 cm²/Vs. Front-gate and light were used to change the density in the range 1.1-4.2 × 10¹⁰ cm⁻². In these measurements, which are performed in a dilution refrigerator with fields up to 18 T, we rotate the sample in a constant *B* applied almost parallel to the 2DES and record the sample resistance (*R*) as a function of the angle between the 2DES and the direction of *B*.^{3,4} We have performed the measurement at different constant temperatures and different total *B*. If we limit ourselves to small angles, the parallel component of the field (*B*_{||}) remains almost constant during the rotation, while the perpendicular component of the field (*B*_⊥) changes sufficiently to probe the Shubnikov - de Haas (SdH) oscillations (Figure 1(a)). The analysis uses the Dingle formula, Δ*R* ~ ξ sinh ξ, where Δ*R* is the amplitude of the SdH oscillations, ξ ≡ 2π²k_BT/ħω_c, and ω_c = e*B*_⊥/*m*^{*}. By fitting this formula to the experimental data we obtain *m*^{*} at a given parallel field *B*_{||} (Figure 1(b)).

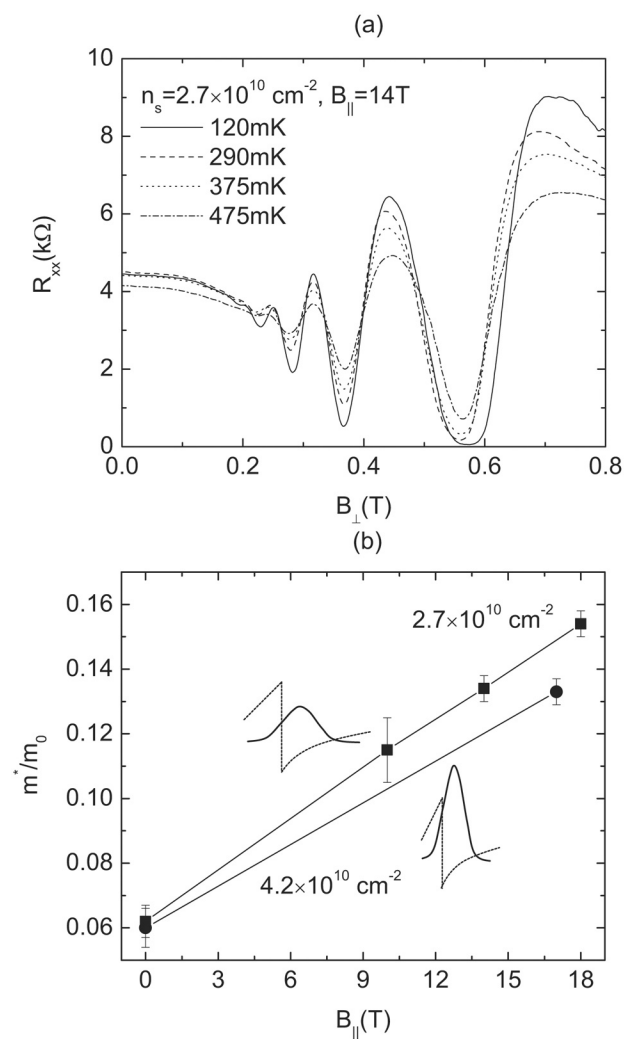


Figure 1. (a) Example of SdH oscillations measured by rotating the sample in a large (14 T) constant magnetic field to introduce a small (<1 T) perpendicular field component. In this type of experiment B_{\parallel} remains constant to better than 1% during the rotation. The measurement was done at different temperatures and the amplitude of the SdH oscillations was fitted to the Dingle formula to obtain the effective mass. (b) Effective mass vs. parallel field at two different 2DES densities. The sketches show the conduction band profile (thin lines) and the charge distribution (thick lines) for the two densities. Note that since we are using a front-gate to reduce the density, the layer thickness increases as the density is reduced. These results show clearly that the effective mass enhancement in parallel magnetic field is larger for the thicker layer.

The results in Figure 1(b) show that m^* increases significantly with the applied B_{\parallel} . The data also demonstrate that the rate at which m^* increases depends on the 2DES layer thickness: the smaller the density, the larger the 2DES layer thickness, and the larger the m^* enhancement. We are currently analyzing our data in detail to determine quantitatively how the m^* enhancement affects the 2DES spin polarization.

Acknowledgements: This work was supported by the NSF and DOE.

- ¹ Abrahams, E., *et al.*, *Rev. Mod. Phys.*, **73**, 251 (2001).
- ² Okamoto, T., *et al.*, *Phys. Rev. Lett.*, **82**, 3875 (1999); Yoon, J., *et al.*, *Phys. Rev. Lett.*, **84**, 4421 (2000); Vitkalov, S.A., *et al.*, *Phys. Rev. Lett.*, **87**, 086401 (2001).
- ³ Tutuc, E., *et al.*, *Phys. Rev. Lett.*, **86**, 036805 (2001).
- ⁴ Tutuc, E., *et al.*, *Phys. Rev. Lett.*, **86**, 036805 (2001).
- ⁵ Das Sarma, S., *et al.*, *Phys. Rev. Lett.*, **84**, 5596 (2000).
- ⁶ Salis, G., *et al.*, *Phys. Rev. B*, **58**, 1436 (1998).

Electron Spin Relaxation Mechanisms of Phosphorus-Doped Silicon

van Tol, J., NHMFL

Brunel, L.-C., NHMFL

Bortolus, M., NHMFL

Phosphorus-doped silicon has been suggested as a prime candidate for the realization of quantum computers. This shallow donor site has an electron spin $S = \frac{1}{2}$ which is coupled to the ^{31}P nuclear spin of $I = \frac{1}{2}$, and either the electron or nuclear spins or both of them could serve as qubits in a quantum computer. One of the main attractions of this system is the possibility of qubit manipulation. Microwave and radio frequency pulses provide a contactless method for the manipulation of the electron and nuclear spins respectively, while electric fields can be used to tune spin-spin interactions. Another reason why this system is seen as a serious candidate for a future quantum computer are the extremely long electron spin relaxation times that were revealed by the pioneering work by G. Feher¹ in the fifties. The longitudinal spin-relaxation time T_{1e} becomes of the order of minutes at liquid helium temperatures, and the requirement that the quantum system should be well isolated from its surroundings seems to be satisfied.

Little has been done regarding the magnetic properties of Si:P since Feher's work, and the proposals concerning a Si-based approach rely on a precise knowledge of the exchange interactions and relaxation mechanisms. In particular, the longitudinal relaxation time T_{1e} and the transversal relaxation time T_{2e} in Si:P are dependent on dopant concentration, strain, temperature, magnetic field, and the presence of ^{29}Si $I = \frac{1}{2}$ nuclear spins. We have initiated a study of the T_{1e} and T_{2e} relaxation times of Si:P at 9.5 and 95 GHz in the 5 K to 20 K range. The results for a Si:P sample with $[\text{P}] = 3 \times 10^{15}$ are shown in Figure 1. It is found that both T_{1e} and T_{2e} are identical for 95 GHz (3.4 T) and 9.7 GHz (0.35 T) in the temperature range studied. Over the measured temperature range the T_{1e} varies by almost 7 orders of magnitude, and a thermally

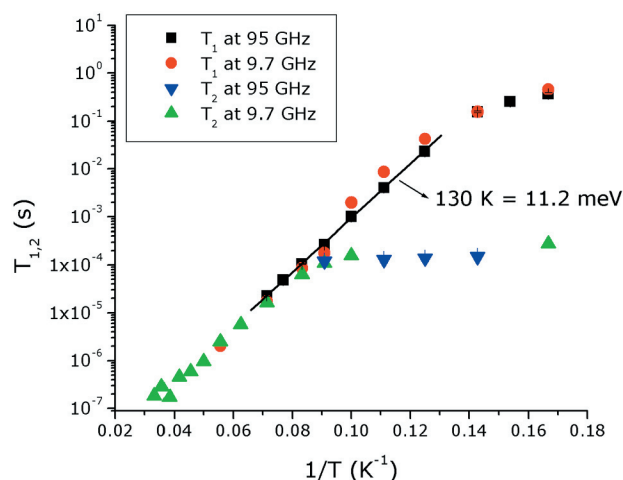


Figure 1. The T_1 and T_2 relaxation times of the electron spin associated with the Phosphorus shallow donors at 0.35 T (9.7 GHz) and 3.4 T (95 GHz). $[P] = 3 \times 10^{15}/\text{cm}^3$.

excited relaxation process with an activation energy of 130 K can characterize its temperature-dependence. This corresponds to the energy of the first excited state of the shallow donor, located just below the conduction-band. The spin-spin or transversal relaxation time T_{2e} is equal to T_{1e} at temperatures above 12 K, but below that temperature it tends to level off at a value of around 100 to 200 μs , and is not single-exponential. It appears that the T_{2e} is limited by the relaxation of the ^{29}Si (4.7% natural abundance) nuclear spins. This loss of electron-spin coherence is a serious drawback for quantum computing applications, and a study of these qubit candidates in silicon with different isotope concentrations and that of other impurities would be very useful.

Acknowledgements: This work was supported by a PEG grant from the Florida State University Research Foundation.

[†] Feher, G., *Phys. Rev.*, **114**, 1219 (1959); Feher, G., *et al.*, *Phys. Rev.*, **114**, 1245 (1959).

Evolution of the Electron Localization in a Non-Conventional Alloy System $\text{GaAs}_{1-x}\text{N}_x$ Probed by High Magnetic Field Photoluminescence

Wang, Y.J., NHMFL

Wei, X., NHMFL

Zhang, Y., National Renewable Energy Laboratory

Mascarenhas, A., National Renewable Energy Laboratory

Xin, H.P., Univ. of California at San Diego, Electrical and Computer Engineering

Hong, Y.G., UCSD, Electrical and Computer Engineering

Tu, C.W., UCSD, Electrical and Computer Engineering

The dilute nitrogen $\text{GaAs}_{1-x}\text{N}_x$ alloy has been extensively studied both theoretically and experimentally over the past few years because of its important applications in electro-optics and interesting fundamental physical properties created by the doping of nitrogen. It has been found that doping nitrogen into GaAs greatly reduces the band gap of GaAs.^{1,2} The microscopic origin for the band gap reduction in $\text{GaAs}_{1-x}\text{N}_x$, however, has been intensively debated in recent years. The most critical issue has been about which factor, the host-impurity interaction or the impurity-impurity coupling, plays the major role.

In order to better understand the nature of various nitrogen induced bound states, the impurity-host interaction, and the extent to which the wisdom for conventional alloys is still applicable to this “unconventional” alloy system, we have carried out magneto photo-luminescence (PL) measurements on a set of $\text{GaAs}_{1-x}\text{N}_x$ samples ($0.1\% < x < 2.5\%$).

Figure 1 shows waterfall plots of magneto PL spectra of $\text{GaAs}_{1-x}\text{N}_x$ at four typical compositions with $x = 0.1\%$, 0.22% , 1.1% and 1.3% in magnetic fields up to 30 T. These samples can be roughly divided into two groups: $x < 0.7\%$ and $x > 1\%$, according to the distinct differences in their spectra and response to the magnetic field. For $x < 0.7\%$, as shown in Figure 1 (a) and (b), many transitions with discrete energies were observed at zero magnetic field. Comparing with previously published results, these transitions are identified to be nitrogen induced bound states. When the applied magnetic field is increased, the positions of these impurity transitions do not shift with magnetic field, indicating that they originate from strong localized states of “deep” impurity centers. Starting from around 10 T, however, at the high-energy edge of the spectrum, a new feature emerges with increasing magnetic field and becomes a well-developed peak at 30 T. Such a new PL feature, hereafter referred to as G, exists for all

the dilutely doped samples (with $x < 0.7\%$) studied in this work. For $x > 1\%$, the discrete impurity-like transitions observed in the low N composition samples are no longer observable; instead a broad band becomes the only feature in the spectra. Figure 1 (c) and (d) show the PL spectra for two typical x values of 1.1 % and 1.3 %. It is clear that the peak position of the broad band shifts to the higher energy with increasing magnetic field at a significantly faster rate than for the low x samples, resembling the behavior for conventional alloys.

From our experimental results, we have learned that: for $x < 0.7\%$, the transition energies for many nitrogen related bound states remain stationary up to 30 T, revealing that they are highly localized states; a new optical transition, G, is observed at the onset of the localized to delocalized transition region in the energy spectrum, showing very a small diamagnetic shift and thus a weak delocalization. For $x > 1\%$, a broad optical transition band is observed with a diamagnetic shift similar to that in a conventional semiconducto alloy, exhibiting extended host-state-like behavior. Our results suggest a complex interaction between nitrogen impurities and the GaAs host.

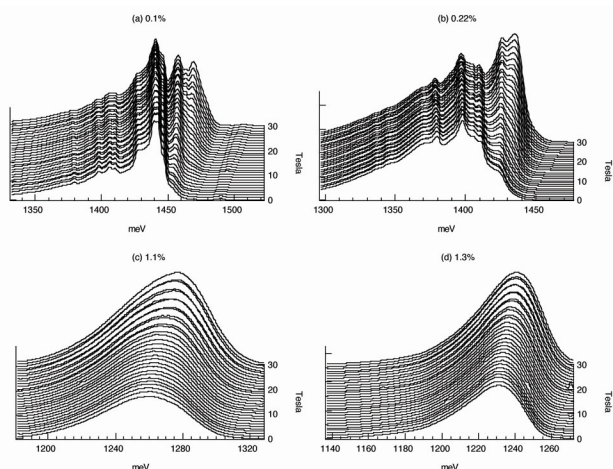


Figure 1. Waterfall plots of PL spectra of GaAs_{1-x}N_x at magnetic field up to 30 T: (a) $x = 0.1\%$, (b) $x = 0.22\%$, (c) $x = 1.1\%$, and (d) $x = 1.3\%$.

¹ Weyers, M., *et al.*, *Jpn. J. Appl. Phys.*, **31**, L853 (1992).

² Zhang, Y., *et al.*, *Phys. Rev. B*, **63**, R161303 (2001).

TEM Characterizations of Co Doped TiO₂ Thin Films by Pulsed Laser Deposition

Xin, Y., NHMFL

Stampe, P.A., Florida A&M Univ., Physics

Kennedy, R.J., Florida A&M Univ., Physics

Spintronics, which utilizes not only charges but also their spins, has become an emerging area of great interests due to its huge potential device applications.¹ Diluted magnetic semiconductors² have attracted enormous attention and intensive research, among them is the optically transparent semiconductor TiO₂ doped with Co showing room temperature ferromagnetism.³

Thin film growth of TiO₂ with Co doping has shown various microstructures and physical properties. The magnetic properties critically depend on the Co distribution into TiO₂ lattice, which varies widely with growth conditions. Therefore it is indispensable to study the microstructures of these thin films by transmission electron microscopy (TEM). Here we report the TEM characterization of the microstructure of these thin films grown on different substrates by pulsed laser deposition (PLD). The samples were grown on single crystal substrates of LaAlO₃, SrTiO₃, and Al₂O₃ at a substrate temperature of 750°C and a background pressure of 1m Torr. The target is made of well mixed powder of TiO₂ with 7% Co after pressing and sintering. The growth rate was about 20 nm/min. A Jeol-2010 microscope operated at 200 kV with a point resolution of 0.23 nm and a Ge energy dispersive spectroscopy (EDS) detector was used.

Figure 1 shows a TiO₂:7%Co thin film grown on LaAlO₃ substrate. The film shows single crystal diffraction pattern of anatase [011] with many round shaped islands protruding out of the surface. The composition analysis by EDS shows that Co is not into the anatase film but segregates onto the surface of the islands, and it was found by nano-diffraction that Co forms as Co metal particles.

Figure 2 gives the microstructures of the film on SrTiO₃ substrate. The left image shows the top portion of the film, and it is comprised of rutile TiO₂ particles with about 100 nm diameter. Co goes into the rutile particle with varied content. The right image shows the part of the film closer to the substrate surface, and it is anatase phase containing very little Co.

Figure 3 is the TEM data from a film on (001)Al₂O₃ substrate. From the diffraction pattern, the film has very textured structure containing both rutile and anatase phase. The grains are quite small, about 20 nm in size. EDS

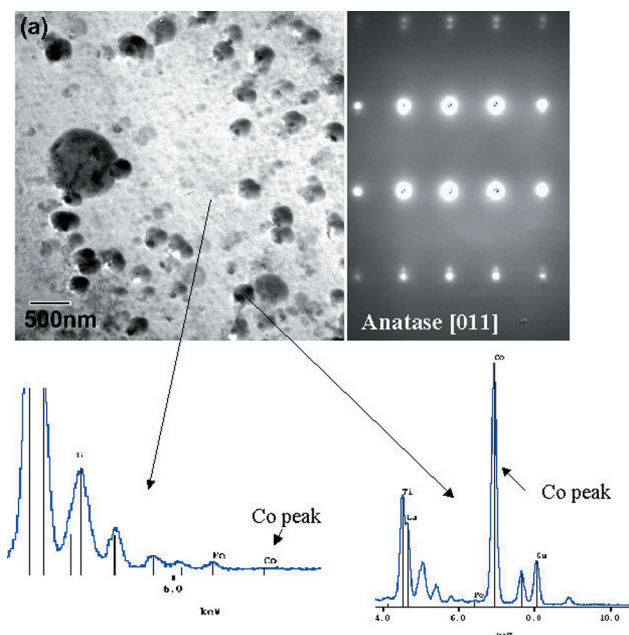


Figure 1. TEM bright field image, diffraction, and EDS spectra from a TiO_2 film grown on (001) LaAlO_3 .

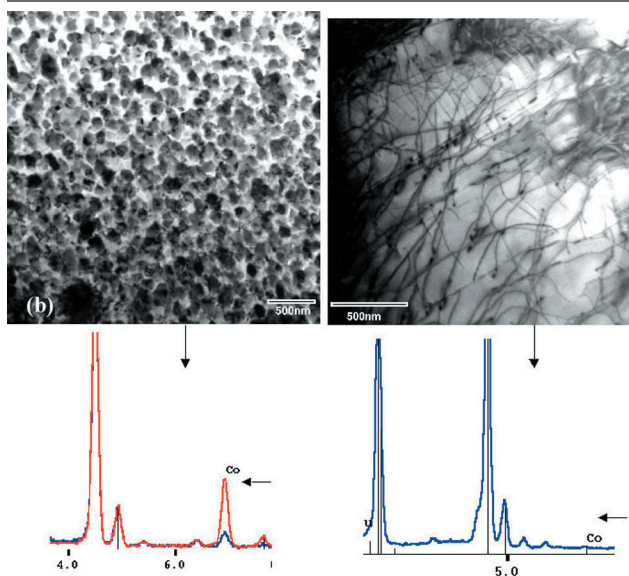


Figure 2. TEM image of a film grown on (001) SrTiO_3 and the corresponding EDS spectra.

analysis indicates an even distribution of Co in the film without any Co clusters.

Three films are all ferromagnetic with different magnetic moment.⁴ From the TEM studies, we can see that the microstructures vary differently with different growth conditions, such as different lattice mismatched substrate and chamber oxygen partial pressure. TiO_2 mainly has two phases, one is the stable rutile phase, and the other the metastable anatase phase. It seems that Co easily goes

into rutile crystal structure than the anatase phase for these PLD thin films. For the anatase film, the ferromagnetic properties may originate from the Co metal clusters on the film surface, in contrast to the rutile phase. It is suggested from molecular beam epitaxy (MBE) growth of these films⁵ that a uniform distribution of Co in anatase films is obtained at a very slow growth rate (0.6 nm/min), while faster growth rate results in rutile phase crystals where Co diffuses and segregates to. The growth rate of the PLD method is exceedingly faster than the MBE growth, therefore Co only goes into rutile phase as observed. X-ray absorption spectroscopy has shown in the Co doped anatase films that Co substitutes Ti in the anatase lattice and has a +2 oxidation state.⁵

Future work will be concentrated on the Co distribution in the rutile phase and their electronic structures using electron energy loss spectroscopy in a TEM.

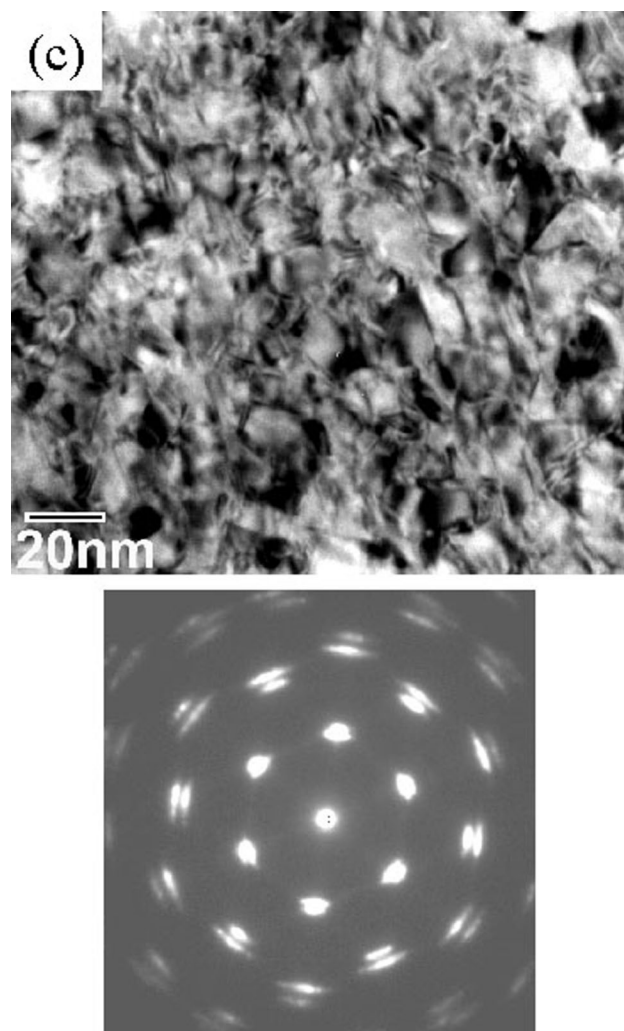


Figure 3. TEM image and diffraction from a film grown on Al_2O_3 .

- ¹ Wolf, S.A., *et al.*, *Science*, **294**, 1488 (2001).
- ² Ohno, H., *Science*, **281**, 951-956 (1998).
- ³ Matsumoto, Y., *et al.*, *Science*, **291**, 854 (2001).
- ⁴ Stampe, P.A., *et al.*, *J. App. Phys.*, **92**, 7114 (2002).
- ⁵ Chambers, S.A., *Thin Sol. Film*, **418**, 197-210 (2002).

Magneto-Optics of Two-Dimensional Electron Gas in ZnSe Quantum Wells in High Magnetic Fields

Yakovlev, D.R., Experimentelle Physik 2, Universität Dortmund, Germany

Astakhov, G.V., Physikalisches Institut der Universität Würzburg, Germany

Crooker, S.A., NHMFL/LANL

Ossau, W., Physikalisches Institut der Universität Würzburg, Germany

The optical properties of a two-dimensional electron gas (2DEG) in a ZnSe/(Zn, Be, Mg)Se quantum well structure have been examined by means of photoluminescence and reflectivity techniques in external magnetic fields up to 50 T. Due to the modulation doping of the barriers with the donors the density of the 2DEG in a quantum wells was $n_e = 5 \times 10^{11} \text{ cm}^{-2}$. For this structure, the Fermi energy of the two-dimensional electron gas (of 7.7 meV) falls in the range between the trion binding energy (about 5 meV) and the exciton binding energy (30 meV), which keeps the dominating role of Coulombic interactions between electrons and photoexcited holes.

We observe that most system parameters measured in magneto-optical spectra (e.g. energy position of line maxima, linewidth, circular polarization degree) exhibit nonmonotonic behavior (peaks, deeps, or spikes) at integer filling factors of the 2DEG. This can be related to the specifics of electron screening in the strongly correlated electron gas.

Strong resonance has been found in reflectivity spectra in vicinity to the high-energy side of photoluminescence band, i.e. at energies that are often related to the so-called "Fermi edge singularity," the transition involving photoholes from the valence band and 2DEG electrons from the vicinity of the Fermi level. We conclude from our data that the qualitative assignment of this transition is valid, but many more details should be clarified before we will get a consistent scenario of the modification of optical spectra with increasing electron density.

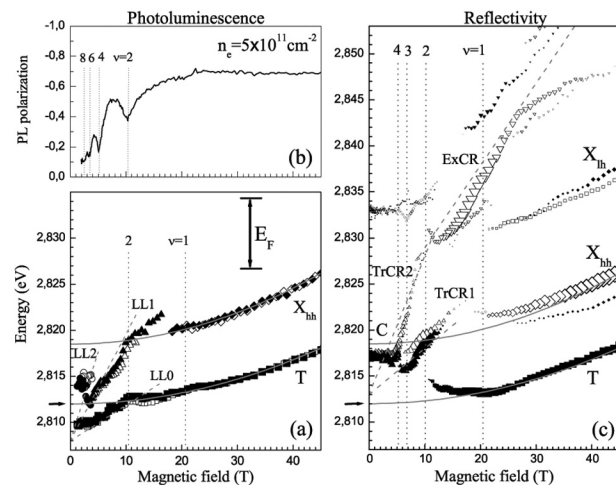


Figure 1. Experimental data of magnetic field behavior of optical spectra in a 67-Å-thick ZnSe/Zn_{0.82}Be_{0.08}Mg_{0.10}Se QW with $n_e = 5 \times 10^{11} \text{ cm}^{-2}$.

- (a) Energies of PL maxima vs. magnetic field strength of detected in σ^+ (open symbols) and σ^- (closed symbols) polarizations. Exciton (X_{hh}) and trion (T) diamagnetic shifts for an undoped QW of the same width are shown by solid lines. They are slightly shifted in energy positions for comparison with the relevant QW. Dashed lines show Landau level fan (LL0, LL1, and LL2) of electron with effective mass $m_e = 0.15m_0$. Arrow indicates the energy of "bare" charged exciton at zero magnetic field, taken from solid line. Dotted lines indicate magnetic fields of integer filling factors.
- (b) Circular polarization degree of the low energy PL line as a function of magnetic fields. Dotted lines indicate location of even filling factors.
- (c) Energies of reflectivity lines vs. magnetic field strength detected in σ^+ (open symbols) and σ^- (closed symbols) polarizations. Intensities of resonances are displayed by a size of symbols. Similar to (a) exciton (X_{hh}) and trion (T) diamagnetic shifts in undoped QW are shown by solid lines. Dashed curves are linear fittings for trion-cyclotron resonances (TrCR) and for exciton-cyclotron resonance (ExCR).

Results of this project have been reported by D.R. Yakovlev as an invited talk at the NATO Workshop on "Optical Properties of 2D Systems with Interacting Electrons," June 2002, St. Petersburg, Russia. They are also included in the following publications:

1. W. Ossau, D.R. Yakovlev, G.V. Astakhov, A. Waag, C.J. Meinig, H.A. Nickel, B.D. McCombe, and S.A. Crooker, *Physica E*, **12**, 512 (2002).
2. W. Ossau, G.V. Astakhov, D.R. Yakovlev, S.A. Crooker, and A. Waag, *Proc. 26th IC on the Physics of Semiconductors*, Edinburgh, UK 2002, publication on CD.
3. D.R. Yakovlev, G.V. Astakhov, W. Ossau, S.A. Crooker, and A. Waag, *Proc. NATO workshop on Optical Properties of 2D Systems with Interacting Electrons*, June 2002, St. Petersburg, Russia, NATO series book.

Reentrant Insulating Phase Near $\nu = 1/3$ Fractional Quantum Hall Effect in a Two-Dimensional Electron System

Yang, I., Univ. of Chicago, Physics

Kang, W., Univ. of Chicago, Physics

Hannahs, S.T., NHMFL

Pfeiffer, L.N., Lucent Technologies

West, K.W., Lucent Technologies

We have observed an unexpected reentrant insulating phase around the $\nu = 1/3$ fractional quantum Hall effect (FQHE) state in a two-dimensional electron (2DES) system.¹ The 2DES in question is found in a GaAs/AlGaAs quantum well whose narrow width produces a tight vertical confinement of the electronic wave function. The experiment was performed using a modulation doped AlGaAs/GaAs quantum well 80-Å wide. The density of the sample was $n = 1.1 \times 10^{11} \text{ cm}^{-2}$ with a low temperature mobility of $\mu = 2.56 \times 10^5 \text{ cm}^2/\text{Vs}$. In spite of its low mobility, we observed a clear sequence of transitions to an insulator, then to the $\nu = 1/3$ FQHE state, and then back to an insulating phase in a fashion reminiscent of the Wigner crystalline regime in other two-dimensional systems.

Significance of the observed reentrant behavior in the 2DES in a NQW derives from the fact that the observed sequence of insulator-FQHE-insulator transitions is strikingly reminiscent of the transitions found in high mobility 2DES. Previous studies of 2DES under high magnetic fields have shown that the reentrant behavior arising from competition from the FQHE liquid and Wigner solid is a universal feature prior to the entry into the Wigner crystalline regime in two-dimensional semiconductors.² Strong resemblance to other two-dimensional systems in the Wigner crystalline regime leads to an intriguing prospect that the reentrant behavior in the NQW is driven by the same physics that is responsible for the reentrance in high mobility 2DES. These results point to an intriguing interplay of disorder and interaction in the Wigner crystalline regime associated with the vertical confinement.

We also detect a clear evidence for a critical point in the initial transition into the reentrant insulating phase. The transition into the reentrant insulating phase appears to be a continuous phase transition with an unambiguous critical point at $B = B_c$ where ρ_{xx} approaches a constant in the limit of zero temperature. The value of ρ_{xx} at B_c is $25.4 \text{ k}\Omega/\text{T}$ close to h/e^2 . Scaling analysis of the ρ_{xx} data near the critical point shows that ρ_{xx} can be plotted in terms of the well-known function of $|B - B_c|T^\kappa$ where $\kappa = 0.42$. Existence of the critical behavior is indicative of a divergent length scale as the transition is approached from either the insulating or the FQHE phase. Presence of a continuous phase transition may come as a consequence of disorder-induced broadening of the first order transition between the crystalline and the liquid states.

¹ Yang, I., *et al.*, submitted to *Phys. Rev. Lett.*

² Jiang, H.W., *et al.*, *Phys. Rev. Lett.*, **65**, 633 (1990).

